EVOLUTION OF A REACTION CENTER IN AN EXPLOSIVE MATERIAL

T. L. Jackson*, A. K. Kapila# and D. S. Stewart**

Abstract

Experimental observations of ignition in explosive systems demonstrate that as a rule, combustion first sets in at small, discrete sites where inherent inhomogeneities cause chemical activity to proceed preferentially and lead to localized explosions. Combustion waves propagating away from these "reaction centers" eventually envelope the remaining bulk.

This study examines the spatial structure and temporal evolution of a reaction center for a model involving Arrhenius kinetics. The center, characterized by peaks in pressure and temperature with little diminution in local density, is shown to have one of two possible self-similar structures. The analysis employs a combination of asymptotics and numerics, and terminates when pressure and temperature in the reaction center have peaked.

* Institute for Computer Applications in Science and Engineering
NASA Langley Research Center, Hampton, Virginia 23665

Department of Mathematical Sciences
Rensselaer Polytechnic Institute, Troy, New York 12180-3590

** Department of Theoretical and Applied Mechanics
University of Illinois, Urbana, Illinois 61801

This work was supported by the U.S. Army Research Office, by the National Aeronautics and Space Administration under NASA Contract NAS1-18107, and by the Los Alamos National Laboratories under Contract DOE-LANL-9XR6-5128C1.

1. Introduction

This paper descibes, mathematically, the birth and growth of a reaction center, or localized thermal explosion, in an explosive material. The material is treated as an ideal, compressible, reacting fluid, and as such is described by the equations of reactive gas dynamics, i.e., the Euler equations with chemistry. This treatment is appropriate not only for mixtures of reacting gases but also for condensed explosives when the characteristic reaction and acoustic times are much too short for diffusion to be significant.

Experimental observations on combustion initiation in explosive systems, in shock tubes and elsewhere, have demonstrated conclusively that spatially homogeneous initiation is essentially an unattainable ideal. In fact, ignition first sets in locally, in small volume elements at discrete sites, where chemical reaction proceeds preferentially due to spatial inhomogeneities in the system. In due course, combustion waves originating from localized explosions occuring at these "reaction centers" or "exothermic centers" envelope the entire reacting mass. The role played by these sites as precursors of more dramatic combustion phenomena is revealed with unsurpassed clarity in Urtiew and Oppenheim's [1] photographic records of deflagration-to-detonation transition in a Hydrogen-Oxygen mixture confined to a tube. These photographs show that as the deflagration travels down the tube, it accelerates and evolves into a highly contorted turbulent flame, preceded by a precursor shock. Eventually, an exothermic center is formed in the trapped, unreacted compressed gas which is captured between the

flame and the shock. The localized explosion in this center creates a blast wave which propagates through the preconditioned mixture behind the precursor shock and ultimately evolves into a fully-developed detonation. The same feature appears in other modes of detonation-initiation in gases, as well as in other geometric configurations.

Experiments on liquid and solid explosives have also documented the role of reaction centers as ignition kernels. Shock-initiation studies on Nitromethane, a sensitive liquid explosive, are but one example. In these experiments, conducted by Campbell, Davis and Travis [2], an inert piston is driven impulsively into the explosive, and it is found that after the elapse of an "induction period", an ignition event occurs in a reaction center at the piston face, ultimately giving rise to a detonation.

The early analyses of reaction-center dynamics are due to Zajac and Oppenheim [3] and Meyer and Oppenheim [4]. In these studies the reaction center is assumed to be a spatially homogeneous source of chemical energy, capable of expansion and separated from its inert surroundings by an impermeable barrier, across which only momentum transfer can occur. Either by prescribing a specific reaction scheme, or by specifying an energy release profile within the center, the above authors were able to compute the resulting pressure pulse.

In this paper the reaction center is treated as part and parcel of the reacting medium rather than an isolated entity in an inert atmosphere, and is found to have a definite spatial structure. The aim of this paper is to describe this structure and

to study its temporal evolution in a plane, one-dimensional framework, under the asssumption that the explosive undergoes a single, one-step, first-order, irreversible chemical reaction of the Arrhenius type. One may argue that the simple overall kinetic scheme adopted here is too idealized to be realistic. However, for large activation energies, the kinetics does capture an essential attribute of most combustion systems, namely, a reaction rate which accelerates rapidly with increase in temperature. Thus the model is quite appropriate for studying problems, such as the one at hand, which owe their genesis to the interaction between gasdynamics and chemical heat release for rates which are highly sensitive functions of the local thermodynamic state. One must reiterate, however, that the specific results obtained here are peculiar to the model adopted; extensions to more complicated models including elaborate kinetic schemes or complex material properties will no doubt change the character of the reaction-center. Indeed, as Stewart [5] has shown, kinetics may influence the site and moment of birth of the reaction center, while multiple hot spots may result as a consequence of variations in the physical properties of the explosive.

In this study the configuration of the system is so prescribed as to provoke the development of a single hot spot, and this can be accomplished in a variety of ways. For example, the shock-induced thermal-runaway studies of Clarke and Cant [6] and Jackson and Kapila [7] considered a semi-infinite expanse of gas ignited by a piston-driven shock, thereby creating a raction center at the piston face. Instead, the present work assumes that the gas is

confined between two parallel planes, and that its initial state possesses a slight spatial nonuniformity. (In a practical situation these non-uniformities may be caused by a variety of factors, such as turbulence, interacting pressure waves, or, in the case of condensed explosives, material imperfections.) The mathematical model leads to an initial-boundary value problem for the equations of reactive gasdynamics. An asymptotic solution is developed in the limit of large activation energy, and the analysis is carried as far as the end of the localized explosion within the center. The subsequent birth of a reaction wave and its propagation will be the subject of a future publication.

The temporal evolution of the explosion occurs in two stages. In the induction stage the state of the material is a small perturbation of the initial state and the underlying physical processes are those of linearized acoustics coupled to a weak but nonlinear chemical reaction. The reduced equations require a numerical solution (see [5], [6] and [7]) which exhibits local thermal runaway, characterized by local unboundedness of the perturbation quantities at a finite time.

Induction is followed by the explosion stage, whose temporal extent is exceedingly short compared to the induction period, and which consists of several distinct spatial zones. There is the outer frozen zone, in which the state of the explosive remains essentially the same as that at the end of the induction stage. This is distinct from the rapidly shrinking inner zone, or hot spot, in which intense chemical activity leads to an explosive growth of temperature and pressure, ultimately limited only by the

consumption of the reactant. To leading order the hot spot is a constant-density, spatially-homogeneous thermal explosion. Its spatial structure is described at the next order by the coupling of chemistry with linearized gasdynamics, but now the linearization is about an atmosphere undergoing a spatially homogeneous thermal explosion. As the layer shrinks, it recedes away from the frozen zone, thereby creating an expanding zone of transition. This new zone is also effectively frozen in time, but in contrast with the outer frozen zone, temperature variations across it are substantial.

Although highly nonlinear, the explosion stage is amenable to analysis because in it, gasdynamics is of secondary importance; temporal variations are much too rapid for the material to undergo significant expansion.

For the specific reaction scheme under consideration it is found that the reaction center can have one of two posible spatial structures, depending upon the initial conditions. The two structures are characterized by the temperature profile within the hot spot possessing a sharp peak or a rounded peak (Figure 1). The former typifies hot spots originating at boundaries (e.g., a piston face), and the latter those occuring in the interior of the vessel. These structures, which will be referred to as the "Type B" (boundary-type) or "Type I" (internal-type), are both self-similar. Type B is described below in detail, with only the results for type I given in section 6. In addition to these two structures there exists a third, described briefly in the Appendix; it is singular and corresponds to very special initial conditions.

The specific configuration under study here was also examined, with similar methods, by Poland and Kassoy [8]. Their analysis differs from ours in one crucial respect; they considered the distinguished limit in which the spatially homogeneous induction time at the initial state and the conduction time across the vessel are of the same order, i.e., the Frank-Kamanetskii number δ is of order unity, albeit supercritical. In our analysis the induction time is comparable to the acoustic time across the vessel, i.e., δ is very large. Such would be the case when the explosive environment has been preconditioned so that the initial reaction rate is very rapid.

2. The Basic Equations, and Setup

The equations of motion for plane, one-dimensional, reactive flow of an ideal gas or a material with a polytropic equation of state are [9]

$$\rho_t + u\rho_x + \rho u_x = 0, \tag{2.1a}$$

$$\rho(u_t + uu_x) + (1/\gamma)p_x = 0, \tag{2.1b}$$

$$\rho(T_t + uT_x) + [(\gamma-1)/\gamma](p_t + up_x) = \beta w, \tag{2.1c}$$

$$\rho(Y_t + uY_x) = -w, \tag{2.1d}$$

$$p = \rho T, \tag{2.1e}$$

where

$$w = [1/(\beta\theta)]\rho Y \exp(\theta - \theta/T). \tag{2.1f}$$

Here p, ρ, T, u and Y are, respectively, the gas pressure, density, temperature, velocity and reactant mass fraction. The variables have been made dimensionless with respect to a constant dimensional reference state $\tilde{p}$, $\tilde{\rho}$, $\tilde{T}$ and $\tilde{Y}$. Velocity is referred to the acoustic speed $\tilde{c}$, defined by

$$\tilde{c} = [\gamma\tilde{p}/\tilde{\rho}]^{1/2},$$

time to $\tilde{t}$, the homogeneous induction time at the reference state (derived from classical explosion theory for large activation energy) and length to $\tilde{c}\tilde{t}$. The diffusion terms have been left out because they are much too small to play a role in the problem under study. The dimensionless parameters appearing above are the specific-heats ratio (or polytropic exponent) γ, the chemical heat release β and the activation energy θ.

Let the material be confined to the interval $0 < x < \ell$. At the walls the appropriate boundary conditions are

$$u(0,t) = u(\ell,t) = 0. \tag{2.2}$$

The initial state of the gas is taken to be a small, $O(\theta^{-1})$ perturbation of the spatially homogeneous and stationary reference state, i.e.,

$$u(x,0) = \theta^{-1}u_1(x,0), \tag{2.3a}$$

$$\Phi(x,0) = 1 + \theta^{-1}\Phi_1(x,0) \text{ for } \Phi = T, p, Y \text{ and } \rho, \tag{2.3b}$$

where $u_1(x,0)$ and $\Phi_1(x,0)$ are assumed to be given. Note that

(2.3c) $$\rho_1(x,0) = p_1(x,0) - T_1(x,0)$$

in accordance with the equation of state (2.1e). An asymptotic solution of the initial-boundary-value problem (2.1)-(2.3) is sought in the limit $\theta \to \infty$, with β and γ fixed and O(1), until the localized explosion has reached completion. The various stages of evolution are detailed in the following sections.

3. The Induction Stage

In the initial stage the state of the gas remains an $O(\theta^{-1})$ perturbation of the reference state. During this period, referred to as the induction stage, one therefore seeks the expansions

(3.1) $$u \sim \theta^{-1}u_1 + \ldots, \quad \Phi \sim 1 + \theta^{-1}\Phi_1 + \ldots,$$

for $\Phi = T,\ p,\ Y$ and ρ

which, upon substitution into the set (2.1) yield the leading-order disturbance equations

(3.2a) $$(\partial/\partial t \pm \partial/\partial x)(p_1 \pm \gamma u_1) = \gamma \exp(T_1),$$

(3.2b) $$\partial/\partial t[T_1 - \{(\gamma-1)/\gamma\}p_1] = \exp(T_1),$$

(3.2c) $$\rho_1 = p_1 - T_1, \quad \partial Y_1/\partial t = -(1/\beta)\exp(T_1).$$

Except for the nonlinear source term, eqns. (3.2a,b) are simply those of linearized acoustics in a uniform atmosphere. It is a

simple matter to integrate them along the characteristics, as was done in [5], [6] and [7]. During induction it is enough to concentrate on the variables T_1, p_1 and u_1, because once they are known, the first eqn. in (3.2c) yields ρ_1 while the second, combined with (3.2b) and integrated, determines Y_1 according to the expression

$$(3.2d) \qquad T_1 - [(\gamma-1/\gamma]p_1 + \beta Y_1 = T_1(x,0) - [(\gamma-1)/\gamma]p_1(x,0) + \beta Y_1(x,0).$$

Equations (3.2) have been solved numerically for representative values of γ and for a variety of smooth initial conditions and interval lengths ℓ. A high-resolution, adaptive scheme was employed to integrate along the characteristics. All computations displayed thermal runaway, characterized by the unboundedness of T_1 and p_1 at a single location in the interval $[0, \ell]$ at a finite time t_e.

The numerical results can all be summarized by considering two representative cases, for which the initial values of pressure and mass fraction correspond to those at the reference state and the initial velocity is zero.

Thus we consider

$$(3.3a) \qquad p_1(x,0) = Y_1(x,0) = u_1(x,0) = 0,$$

while the initial temperature perturbations are prescribed as

$$(3.3b) \qquad T_1(x,0) = a[1-(x/\ell)] \text{ for type B, } a[1-(x/\ell)^2] \text{ for type I.}$$

In both cases the initial temperature disturbance has a single maximum at $x = 0$, causing it to become the site of thermal runaway. The essential difference between the two cases is that in the first the initial temperature disturbance has a nonzero spatial gradient (sharp peak) and in the second, a zero spatial gradient (rounded peak), at $x = 0$. Thus the first case typifies a hot spot located at the boundary (e.g., the shock configuration discussed in [5], [6] and [7]), and the second an internal hot spot. These will be referred to, respectively, as type-B (boundary) and type-I (internal). Their spatial structures, it turns out, are different.

In the following sections the type-B problem is discussed in detail. The type-I problem can be treated analogously and is, in fact, slightly simpler to analyze; it was deemed sufficient, therefore, to simply state its solution in seaction 6.

We start with Figure 2, which displays the numerical results for the Type-B induction solution. The four graphs there exhibit, respectively, the profiles of T_1, p_1, u_1 and ρ_1 against x for increasing values of t. The curves at the latest time show the solution very close to the blowup time t_e, the time beyond which the integration routine was unsuccessful. An examination of the T_1-solution near blowup reveals that growth is most rapid in a thin boundary layer near $x = 0$. Additional information about this growth is provided by Figure 3, where the function $\exp[-T_1(0,t)]$ is graphed near blowup. The straight-line graph in the figure has slope γ, to the accuracy of the numerical scheme, and a t-intercept equal to the blowup time t_e, allowing one to conclude that

(3.4) $T_1(0,t) \sim -\ell n[\gamma(t_e-t)] + o(1)$ as $t \to t_e$.

Figure 4 displays time plots of the solution at x = 0, and shows clearly that while $T_1(0,t)$ and $p_1(0,t)$ become unbounded, $\rho_1(0,t)$ does not. Therefore, $p_1(0,t)$ must have precisely the same leading-order behavior as $T_1(0,t)$, i.e.,

(3.5) $p_1(0,t) \sim -\ell n[t_e-t] + O(1)$ as $t \to t_e$.

To summarize, the induction stage exhibits the classic logarithmic singularity of spatially homogeneous thermal runaway [10].

4. The Structure of the Boundary-type (type-B) Induction-phase Singularity

Although numerics confirms the existence and the temporal character of thermal runaway, further analysis is needed to determine its spatial structure. Such an analysis would involve coordinate expansions for t near t_e. Accordingly, it is convenient to introduce a new time variable τ via the expression

(4.1) $\tau = t_e-t, \quad \tau > 0.$

Then eqns. (3.2a,b) transform into

(4.2a) $\partial p_1/\partial x - \gamma \partial u_1/\partial \tau = 0,$

(4.2b) $\gamma \partial u_1/\partial x - \partial p_1/\partial \tau = \gamma \exp(T_1),$

(4.2c) $[(\gamma-1)/\gamma]\, \partial p_1/\partial \tau - \partial T_1/\partial \tau = \exp(T_1),$

where the dependent variables are now functions of x and τ. The relevant boundary condition is the first of (2.2), re-written as

(4.3) $\qquad u_1(0,\tau) = 0.$

Elementary manipulations on (4.2a,b) and (4.3) yield the following integral, which will prove to be of value later on:

(4.4) $$\mathcal{J}(\tau) \equiv \left[\partial T_1(x,\tau)/\partial x\right]_{x=0} = \mathcal{J}_0 \exp\left[\int_{\tau}^{t_e} \exp(T_1(0,\eta))\,d\eta\right],$$

where $\mathcal{J}(\tau)$ denotes the disturbance temperature gradient at $x = 0$, and $\mathcal{J}_0$ its initial value, i.e.,

(4.5) $\qquad \mathcal{J}_0 = \mathcal{J}(t_e-).$

Recall, from (3.3b), that $\mathcal{J}_0$ vanishes for type I but is negative for type B. Then (4.4) shows that $\mathcal{J}(\tau) \equiv 0$ (rounded peak) for the former and decreases monotonocally to $-\infty$ (sharp peak approaching a cusp) for the latter as $\tau \to 0+$.

We now turn to the analysis of the structure of the induction singularity. As indicated above, it is properly analyzed by seeking separate coordinate expansions as $\tau \to 0$, within the boundary layer and in the region outside. The outer region is governed by the outer limit process

$$x > 0 \text{ and fixed}, \quad \tau \to 0.$$

The boundary layer, on the other hand, corresponds to an inner limit process

$$s > 0 \text{ and fixed}, \quad \tau \to 0,$$

where $s(x, \tau)$ is the spatial coordinate in the boundary layer. The shrinking nature of the layer requires x to vanish under the inner limiting process. If one conjectures that the singularity is locally self-similar, eqns. (4.2a-c) require that s must be defined by

$$s = x/\tau, \tag{4.6}$$

this being the only choice which assigns coequal importance to the x- and τ-derivatives, thereby providing the richest equations for the inner limit.

Henceforth we shall refer to the boundary layer as the hot spot. It will transpire that the scaling (4.6) does not quite span the entire hot spot. Rather, the hot spot is found to have a two-sublayer structure, consisting of a thin central core embedded in a thicker, main body. The various spatial regimes are displayed schematically in Fig. 5. There, H refers to the hot spot and FR to the frozen region outside. Within the hot spot, HC denotes the core and HB the main body.

We shall first examine the core, show that it becomes nonuniform for large s, determine the appropriate scaling and expansions for the main body and demonstrate that the latter merges

smoothly into the outer region. Only one or two terms of the expansions in each region will be computed; continuation to higher orders is straightforward though increasingly complex algebraically.

4.1 The Core HC

The induction-phase equations (4.2a-c), written in the (s,τ) variables, are

$$(4.7a)\qquad (s\partial/\partial s - \tau\partial/\partial\tau)[\gamma T_1 - (\gamma-1)p_1] = \gamma\tau\exp(T_1),$$

$$(4.7b)\qquad (s\partial/\partial s - \tau\partial/\partial\tau)p_1 + \gamma\partial u_1/\partial s = \gamma\tau\exp(T_1),$$

$$(4.7c)\qquad (s\partial/\partial s - \tau\partial/\partial\tau)u_1 + (1/\gamma)\partial p_1/\partial s = 0.$$

It is convenient to isolate the temporal singularity from the spatial structure. Accordingly, we define the structure functions $\mathcal{J}$, $\mathcal{P}$ and $\mathcal{U}$ by setting

$$(4.8a)\qquad T_1 = -\ell n(\gamma\tau) + \mathcal{J}(s,\tau),$$

$$(4.8b)\qquad p_1 = -\ell n(B\tau) + \mathcal{P}(s,\tau),$$

$$(4.8c)\qquad u_1 = \mathcal{U}(s,\tau),$$

where the yet unknown constant B represents a weak influence of the initial conditions on the self-similar boundary layer, and will be determined in due course by matching. Substitution of (4.8) into (4.7) yields the structure equations

$$(4.9a)\qquad s\mathcal{J}_s - \tau\mathcal{J}_\tau + (\gamma-1)\mathcal{U}_s = e^{\mathcal{J}} - 1,$$

(4.9b) $$s(\mathcal{J}_s - \mathcal{Q}_s) - \tau(\mathcal{J}_\tau - \mathcal{Q}_\tau) - \mathcal{U}_s = 0,$$

(4.9c) $$s\mathcal{U}_s - \tau\mathcal{U}_\tau + (1/\gamma)\mathcal{Q}_s = 0,$$

where subscripts denote partial derivatives. The only boundary condition appropriate for the above set is the wall condition

(4.10) $$\mathcal{U}(0, \tau) = 0.$$

In addition, since the initial data are smooth, the structure functions and their s-derivatives are required to be regular in s. Consider the asymptotic expansions

(4.11) $$\Phi \sim \sigma_1(\tau)\Phi_1^{(HC)}(s) + \sigma_2(\tau)\Phi_2^{(HC)}(s) + \ldots$$

$$\text{for } \Phi = \mathcal{J}, \mathcal{Q}, \text{ and } \mathcal{U},$$

as $\tau \to 0$. (In the remainder of this section the superscript HC, which refers to the core of the hot spot, will not be displayed explicitly.) The gauge sequence $\{\sigma_n(\tau)\}$ has not been specified, but a natural choice is provided by the integral relation (4.4), rewritten as

(4.12) $$\mathcal{J}_s(0, \tau) = \mathcal{J}_0\, \tau \exp\left[-\int_{t_e}^{\tau} \{1/(\gamma\eta)\}\exp\{\mathcal{J}(0, \eta)\}d\eta\right]$$

in view of the scaling (4.6) and the prescription (4.8). For small τ the $\mathcal{J}$-expansion in (4.11) allows the above relation to be reduced further to the asymptotic form

(4.13) $$\sigma_1 \mathcal{J}_1'(0) + \ldots = \mathcal{J}_0 \tau^{\lambda} \exp\left[\mathcal{D}(1) - (\mathcal{J}_1(0)/\gamma)\int_0^{\tau} \eta^{-1}\sigma_1(\eta)\,d\eta + \ldots\right],$$

where

(4.14) $$\lambda = (\gamma-1)/\gamma.$$

Recall, from (4.5), that the constant $\mathcal{J}_0$ is nonzero for the Type-B problem. Then, the assumption that $\mathcal{J}_1'(0)$ is nonvanishing (involving no loss of generality) leads to the conclusion

(4.15) $$\sigma_1(\tau) = \tau^{\lambda}$$

if the two sides of (4.13) are to balance at leading order. With σ_1 determined, it can be shown that the expansions (4.11) proceed in powers of τ^{λ}.

Substitution of (4.11) into (4.9) yields the leading-order structure equations for the inner sublayer,

(4.16a) $$(s\,d/ds - \lambda)\mathcal{J}_1 + (\gamma-1)d\mathcal{U}_1/ds = \mathcal{J}_1,$$

(4.16b) $$(s\,d/ds - \lambda)(\mathcal{J}_1 - \mathcal{Q}_1) - d\mathcal{U}_1/ds = 0,$$

(4.16c) $$(s\,d/ds - \lambda)\mathcal{U}_1 + (1/\gamma)d\mathcal{Q}_1/ds = 0,$$

subject to

(4.16d) $$\mathcal{U}_1(0) = 0$$

and regularity. Elimination of $\mathcal{P}_1$ and $\mathcal{U}_1$ from (4.16a-c) leads to the third-order equation

$$(4.17)\qquad [(s^3-s)\mathcal{J}_1']'' + \lambda[1-3s^2)\mathcal{J}_1']' - (s^2-1/\gamma)\mathcal{J}_1'' + (\lambda+1)(3\lambda-4)s\mathcal{J}_1' + (\lambda^2-1)(2-\lambda)\mathcal{J}_1 = 0$$

for $\mathcal{J}_1$, where ' denotes differentiation with respect to s. The points s=0 and s=1 are singular points of this equation and the three linearly independent solutions have the asymptotic behavior

$$1,\ s \text{ and } s\ell ns \text{ as } s \to 0, \text{ and}$$
$$1,\ 1-s \text{ and } |1-s|^{3(\gamma-1)/2\gamma} \text{ as } s \to 1.$$

In general one can expect a one-parameter family of regular solutions to exist, and numerical computations verify that such is indeed the case. A convenient parameter is

$$(4.18)\qquad A = \mathcal{J}_1(0).$$

With $\mathcal{J}_1$ known, $\mathcal{U}_1'$ can be eliminated from (4.16a,b) to obtain a first-order differential equation for $\mathcal{P}_1$ whose regular solution turns out to be

$$(4.19a)\qquad \mathcal{P}_1 = [(\gamma+1/\lambda)/(\gamma-1)]\mathcal{J}_1 - [s^\lambda/\lambda(\gamma-1)]\int \eta^{-\lambda}\mathcal{J}_1'(\eta)d\eta,$$

and then, (4.16c) integrates to give

$$(4.19b)\qquad \mathcal{U}_1 = \mathcal{P}_1'/(\gamma\lambda) - [s^{\lambda}/(\gamma\lambda)]\int_0^s \eta^{-\lambda}\mathcal{P}_1''(\eta)\,d\eta,$$

where regularity has been imposed again. Thus the full solution at this order depends on the single parameter A. Graphs of $\mathcal{J}_1$, $\mathcal{P}_1$ and $\mathcal{U}_1$ for A = 1 are drawn in Figure 6.

At this stage the solution (4.8) has the following expansions in the interior sublayer:

$$(4.20a)\qquad T_1 \sim -\ell n(\gamma\tau) + \tau^{\lambda}\mathcal{J}_1(s) + \ldots,$$

$$(4.20b)\qquad p_1 \sim -\lambda n(B\tau) + \tau^{\lambda}\mathcal{P}_1(s) + \ldots,$$

$$(4.20c)\qquad u_1 \sim \tau^{\lambda}\mathcal{U}_1(s) + \ldots .$$

In order to determine the spatial extent of the core HC one needs the asymptotic behavior of $\mathcal{J}_1$, $\mathcal{P}_1$ and $\mathcal{U}_1$ for large s. This is easily obtained from (4.17) and (4.19), as

$$(4.21a)\qquad \mathcal{J}_1 \sim -A\alpha[s^{(2\gamma-1)/\gamma} + s^{-1/\gamma}(A_{\mathcal{J}}\,\ell ns + B_{\mathcal{J}}) + C_{\mathcal{J}}\,s^{-(\gamma-1)/\gamma} + \ldots],$$

$$(4.21b)\qquad \mathcal{P}_1 \sim -A\alpha[s^{(2\gamma-1)/\gamma} + D_{\mathcal{P}}\,s^{(\gamma-1)/\gamma} + s^{-1/\gamma}(A_{\mathcal{P}}\,\ell ns + B_{\mathcal{P}}) + C_{\mathcal{P}}\,s^{-(\gamma-1)/\gamma} + \ldots],$$

$$(4.21c)\qquad \mathcal{U}_1 \sim -A\alpha[s^{(\gamma-1)/\gamma}(A_{\mathcal{U}}\,\ell ns + B_{\mathcal{U}}) + C_{\mathcal{U}}s^{-1/\gamma} + \ldots].$$

Here α, $B_{\mathcal{J}}$ and $C_{\mathcal{J}}$ are constants with values

$$\alpha = 2.660, \quad B_{\mathcal{J}} = -0.236, \quad C_{\mathcal{J}} = 0.0736$$

obtained by integrating the $\mathcal{J}_1$ equation (4.17) numerically. The

remaining constants appearing above are given by

$$
\begin{aligned}
&A_J = -(2\gamma-1)(\gamma-1)^2/(2\gamma^3), \quad A_\beta = (\gamma+1)A_J/(\gamma-1),\\
&A_u = 2A_J\gamma/(\gamma-1)^2, \quad B_\beta = A_J/(\gamma-1) + (\gamma+1)B_J/(\gamma-1),\\
&B_u = 2B_J\gamma/(\gamma-1)^2 - \gamma(3\gamma-1)A_J/(\gamma-1)^3,\\
&C_\beta = (2\gamma+1)C_J/(2\gamma-2), \quad C_u = -3\gamma C_J/(\gamma-1),\\
&D_\beta = -3C_J\gamma^3/(\gamma-1)^2.
\end{aligned}
\tag{4.22}
$$

The range of validity of the expansions (4.20) can now be determined. For example, substitution of (4.21a) into (4.20a) suggests that the latter becomes nonuniform when

$$\tau^\lambda s^{(2\gamma-1)/\gamma} = O(1), \text{ i.e., } s = O(\tau^{-\mu}),$$

where

$$\mu = (\gamma-1)/(2\gamma-1) \tag{4.23}$$

and the definition (4.14) of λ has been invoked. Correspondingly,

$$x = O(\tau^{\gamma/(2\gamma-1)}) = o(1).$$

The smallness of x indicates that although one has reached the edge of the core HC, the frozen region FR is still far away. The need for a thicker exterior layer, corresponding to the main body of the hot spot, HB, is therefore apparent.

4.2 The Main Body of the Hot Spot, HB

In this layer the appropriate variables are ξ and τ, with ξ defined by

$$(4.24) \qquad \xi = \tau^{\mu} s \equiv x/\tau^{\gamma/(2\gamma-1)}.$$

The expressions (4.8) for T_1, p_1 and u_1 hold again, provided $\mathcal{J}$, $\mathcal{Q}$ and $\mathcal{U}$ are now treated as functions of ξ and τ. The structure equations, obtained from (4.9) by transforming from s to ξ, are

$$(4.25a) \qquad (1-\mu)\xi\mathcal{J}_{\xi} - \tau\mathcal{J}_{\tau} + (\gamma-1)\tau^{\mu}\mathcal{U}_{\xi} = e^{\mathcal{J}} - 1,$$

$$(4.25b) \qquad (1-\mu)\xi(\mathcal{J}_{\xi} - \mathcal{Q}_{\xi}) - \tau(\mathcal{J}_{\tau} - \mathcal{Q}_{\tau}) - \tau^{\mu}\mathcal{U}_{\xi} = 0,$$

$$(4.25c) \qquad (1-\mu)\xi\mathcal{U}_{\xi} - \tau\mathcal{U}_{\tau} + (1/\gamma)\tau^{\mu}\mathcal{Q}_{\xi} = 0.$$

Matching requirements imposed by HC, obtained by substituting (4.21) into (4.20) and then employing (4.24) are

$$(4.26a) \qquad \mathcal{J} \sim -A\alpha\,\xi^{(2\gamma-1)/\gamma} + O(\tau^{2\mu}\,\ell n\tau),$$

$$(4.26b) \qquad \mathcal{Q} \sim -A\alpha\,\xi^{(2\gamma-1)/\gamma} + O(\tau^{\mu}),$$

$$(4.26c) \qquad \mathcal{U} \sim -A\alpha\,\tau^{\mu}\,\xi^{(\gamma-1)/\gamma}[A_{\mathcal{U}}(-\mu\,\ell n\tau + \ell n\xi) + B_{\mathcal{U}}] + O(\tau^{2\mu}), \text{ as } \xi \to 0.$$

Guided by these the HB-solution is sought in the form

$$(4.27a) \qquad \mathcal{J} \sim \mathcal{J}_0^{(HB)}(\xi) + \ldots,$$

$$(4.27b) \qquad \mathcal{Q} \sim \mathcal{Q}_0^{(HB)}(\xi) + \ldots,$$

$$(4.27c) \qquad \mathcal{U} \sim \tau^{\mu}[\ell n\tau\,\mathcal{U}_0^{(HB)}(\xi) + \mathcal{U}_1^{(HB)}(\xi)] + \ldots .$$

(In the remainder of this section the superscript HB will not be displayed explicitly.) Substitution into (4.25) leads to the differential equations

$$(1-\mu)\,\xi\,\mathcal{J}_0' = \exp(\mathcal{J}_0)-1,$$
$$\mathcal{J}_0' - \mathcal{Q}_0' = 0,$$
$$(1-\mu)\,\xi\,\mathcal{U}_0' - \mu\mathcal{U}_0 = 0,$$
$$(1-\mu)\,\xi\,\mathcal{U}_1' - \mu\mathcal{U}_1 = \mathcal{U}_0 - (1/\gamma)\mathcal{Q}_0',$$

whose solutions, subject to the matching requirements (4.26), are

$$\mathcal{J}_0(\xi) = \mathcal{Q}_0(\xi) = -\ln[1+A\alpha\xi^{(2\gamma-1)/\gamma}], \tag{4.28a}$$
$$\mathcal{U}_0(\xi) = -A\alpha\{(\gamma-1)/\gamma^2\}\xi^{(\gamma-1)/\gamma}, \tag{4.28b}$$
$$\mathcal{U}_1(\xi) = A\alpha\,\xi^{(\gamma-1)/\gamma}[\{(2\gamma-1)/\gamma^2\}\{\ln\xi + \mathcal{J}_0(\xi)\} - B_{\mathcal{U}}]. \tag{4.28c}$$

Thus the HB-solution can be written as

$$T_1 \sim -\ln(\gamma\tau) + \mathcal{J}_0(\xi) + \ldots, \tag{4.29a}$$
$$p_1 \sim -\ln(B\tau) + \mathcal{J}_0(\xi) + \ldots, \tag{4.29b}$$
$$u_1 \sim \tau^{\mu}\,[\ln\tau\;\mathcal{U}_0(\xi) + \mathcal{U}_1(\xi)] + \ldots\ . \tag{4.29c}$$

One must consider the behavior of this solution for large ξ in order to assess the spatial extent of the layer HB. This can be done, for example, by substituting the large-ξ behavior of (4.28a) into (4.29a). The result is the expansion

$$T_1 \sim -\{(2\gamma-1)/\gamma\}\ln(\tau^{\gamma/(2\gamma-1)}\xi) - \ln(A\alpha\gamma) + \ldots,$$
$$\text{as } \xi \to \infty,$$

which clearly becomes disordered when $\xi = O(\tau^{-\gamma/(2\gamma-1)})$. Correspondingly, $x = O(1)$, indicating that the edge of the hot spot has now been reached. The next step is to see if the hot spot merges smoothly with the frozen region FR.

4.3 The Frozen Region FR

In the frozen region, where x and τ are the proper variables, the solution can be expanded as

$$\Phi \sim \Phi_0^{(FR)}(x, t_e) + \tau\, \Phi_1^{(FR)}(x) + \ldots, \tag{4.30}$$

$$\text{for } \Phi = T_1,\ p_1 \text{ and } u_1.$$

Here, the leading terms are the numerically obtained limiting values at blowup and the higher-order terms can be computed from (4.2a-c) under the outer limit process. It is a straightforward matter to establish that a match of (4.30) with the HB-solution (4.29a-c) requires the following asymptotic behavior of the frozen solution at blowup:

$$T_1 \sim -\{(2\gamma-1/\gamma)\}\ell n x - \ell n(A\alpha\gamma) + \ldots, \tag{4.31a}$$

$$p_1 \sim -\{(2\gamma-1/\gamma)\}\ell n x - \ell n(A\alpha B) + \ldots, \tag{4.31b}$$

$$u_1 \sim A\alpha^{(\gamma-1/\gamma)}\left[\{(2\gamma-1)/\gamma^2\}[\{-(\gamma-1)/\gamma\}\ell n x + \ell n(A\alpha)] + B_u\right] + \ldots, \text{ as } x \to 0. \tag{4.31c}$$

A careful examination of the numerical solution does, indeed, confirm this behavior. The constants A and B, the only ones yet undetermined, are found by comparing the above expansions with the

numerical solution. The comparison is made at the "edge" of the boundary layer, i.e., for (x,τ) satisfying $\tau \ll 1$, $\tau^{\gamma/(2\gamma-1)} \ll x \ll 1$. It should be emphasized that the structure of the blowup singularity is influenced by the initial conditions only via these constants; otherwise, the solution has a universal, self-similar structure.

4.4 Summary

The near-blowup analysis is now complete, and can be summarized. In the core HC the expansions are

$$T \sim 1 + \theta^{-1}[-\ell n(\gamma\tau) + \tau^{\lambda}\mathcal{J}_1^{(HC)}(s) + \ldots] + \ldots, \tag{4.32a}$$

$$p \sim 1 + \theta^{-1}[-\ell n(B\tau) + \tau^{\lambda}\mathcal{P}_1^{(HC)}(s) + \ldots] + \ldots, \tag{4.32b}$$

$$u \sim \theta^{-1}[\tau^{\lambda}\mathcal{U}_1^{(HC)}(s) + \ldots] + \ldots, \tag{4.32c}$$

where $\mathcal{J}_1^{(HC)}$, $\mathcal{P}_1^{(HC)}$ and $\mathcal{U}_1^{(HC)}$ are defined by (4.17) and (4.19). In the main body of the hot spot, HB, the solution is

$$T \sim 1 + \theta^{-1}[-\ell n(\gamma\tau) + \mathcal{J}_0^{(HB)}(\xi) + \ldots] + \ldots, \tag{4.33a}$$

$$T \sim 1 + \theta^{-1}[-\ell n(B\tau) + \mathcal{J}_0^{(HB)}(\xi) + \ldots] + \ldots, \tag{4.33b}$$

$$u \sim \theta^{-1}[\tau^{\mu}\,\ell n\tau\,\mathcal{U}_0^{(HB)}(\xi) + \tau^{\mu}\,\mathcal{U}_1^{(HB)}(\xi) + \ldots] + \ldots, \tag{4.33c}$$

where $\mathcal{J}_0^{(HB)}$, $\mathcal{U}_0^{(HB)}$ and $\mathcal{U}_1^{(HB)}$ are given by (4.28). In the frozen region FR the expansions take the form

$$T \sim 1 + \theta^{-1}[T_{10}^{(FR)}(x,t_e) + O(\tau)] + \ldots, \tag{4.34a}$$

$$p \sim 1 + \theta^{-1}[p_{10}^{(FR)}(x,t_e) + O(\tau)] + \ldots, \tag{4.34b}$$

(4.34c) $$u \sim 1 + \theta^{-1}[u_{10}^{(FR)}(x,t_e) + O(\tau)] + \ldots,$$

where $T_{10}^{(FR)}$, $p_{10}^{(FR)}$ and $u_{10}^{(FR)}$ are the terminal values of the induction solution, determined numerically.

The remaining variables ρ and Y can be computed, upto $O(\theta^{-1})$, by appealing to the first equation of (3.2c) and (3.2d). The results are

(4.35a) $$\rho \sim 1 + \theta^{-1}[\ell n(Y/B) + \tau^{\lambda}(\mathcal{P}_1^{(HC)} - \mathcal{J}_1^{(HC)}) + \ldots] + \ldots,$$

(4.35b) $$Y \sim 1 + (\theta\beta\gamma)^{-1}[\ell n(A_Y\tau) + \tau^{\lambda}\{(\gamma-1)\mathcal{P}_1^{(HC)} - \gamma\mathcal{J}_1^{(HC)}\} + \ldots] + \ldots$$

in HC,

(4.36a) $$\rho \sim 1 + \theta^{-1}[\ell n(Y/B) + \ldots] + \ldots,$$

(4.36b) $$Y \sim 1 + (\theta\beta\gamma)^{-1}[\ell n(A_Y\tau) - \mathcal{J}_0^{(HB)}(\xi) + \ldots] + \ldots$$

in HB, and

(4.37a) $$\rho \sim 1 + \theta^{-1}[p_{10}^{(FR)}(x,t_e) - T_{10}^{(FR)}(x,t_e) + O(\tau)] + \ldots,$$

(4.37b) $$Y \sim 1 + (\theta\beta)^{-1}[\{(\gamma-1)/\gamma\}p_{10}^{(FR)}(x,t_e) - T_{10}^{(FR)}(x,t_e) + a(1-x/\ell) + O(\tau)] + \ldots,$$

in FR. The constant A_Y appearing in (4.35b) and (4.36b) is given by

(4.38) $$A_Y = \exp[\gamma a + \gamma\ell n\gamma - (\gamma-1)\ell nB].$$

Observe that the hot-spot-solutions (4.32), (4.33), (4.35) and (4.36) break down when $-\ell n\tau = O(\theta)$, signalling the end of the induction stage, and the onset of explosion. The frozen-region-solution, (4.34) and (4.37), suffers no disordering and in fact, becomes increasingly accurate as $\tau \to 0$.

5. The Type-B Explosion Stage

The nonuniformity just encountered decrees that further evolution in the boundary layer occur on the new time scale σ, defined by

$$\tau = e^{-\theta\sigma}. \tag{5.1}$$

For $\sigma = O(1)$ the limit $\theta \to \infty$ corresponds to a time interval of exponential brevity compared to the induction period; its role in the evolution of thermal explosions was first recognized and exploited by Kassoy [10]. The two layers comprising the hot spot must again be examined in turn. In fact, we shall find that as the hot spot continues to shrink, an expanding region of transition (denoted by TR in Figure 5), is created between the hot spot and the frozen region. We shall find that compared to the hot spot, this region is also one of relative chemical inactivity, and has a simple description.

5.1 The Core of the Hot Spot, HC

The spatial coordinate in the core remains s, now written as

$$s = x/\tau \equiv e^{\theta\sigma}\, x,$$

thereby expressing explicitly the continuous shrinkage of the region. In the (s, σ) variables eqns. (2.1) transform into

(5.2a) $$\theta^{-1}\rho_\sigma + s\rho_s + (\rho u)_s = 0,$$

(5.2b) $$\rho[\theta^{-1}u_\sigma + su_s] + (1/\gamma)p_s + \rho u u_s = 0,$$

(5.2c) $$\rho[\theta^{-1}T_\sigma + sT_s] - \{((\gamma-1)/\gamma)[\theta^{-1}p_\sigma + sp_s] + u[\rho T_s - \{((\gamma-1)/\gamma)p_s] = W,$$

(5.2d) $$\rho[\theta^{-1}Y_\sigma + sY_s] + u\rho Y_s = -(1/\beta)W,$$

(5.2e) $$p = \rho T,$$

where

(5.3) $$W = \theta^{-1}\rho Y \exp[\theta(1-\sigma-1/T)].$$

The boundary condition (2.2) is rewritten as

(5.4) $$u(0,\sigma) = 0.$$

At fixed s the solution must match with the induction zone as $\sigma \to 0$. To obtain the necessary conditions one applies the "explosion limit" σ fixed, $\theta \to \infty$ to the HC-solution of the induction stage (4.32), (4.35) to get

(5.5a) $$T \sim 1+\sigma - \theta^{-1}\ell n\gamma + \ldots + \delta[\mathcal{J}_1^{(HC)}(s) + \ldots],$$

(5.5b) $$p \sim 1+\sigma - \theta^{-1}\ell nB + \ldots + \delta[\mathcal{P}_1^{(HC)}(s) + \ldots],$$

(5.5c) $$u \sim \delta[\mathcal{U}_1^{(HC)}(s) + \ldots],$$

(5.5d) $$\rho \sim 1 + \theta^{-1}\ell n(\gamma/B + \ldots + \delta[\mathcal{P}_1^{(HC)}(s) - \mathcal{J}_1^{(HC)}(s) + \ldots],$$

(5.5e) $$Y \sim 1-\sigma/(\beta\gamma) + (\theta\beta\gamma)^{-1}\ell nA_Y + \ldots + \delta(\beta\gamma)^{-1}[(\gamma-1)\mathcal{P}_1^{(HC)}(s) - \gamma\mathcal{J}_1^{(HC)}(s) + \ldots], \text{ as } \sigma \to 0.$$

Here,

(5.6) $$\delta = \theta^{-1}\, e^{-\sigma\theta\lambda},$$

where λ was defined in (4.14) and A_Y in (4.38). These conditions reveal that spatial variations in the explosion stage appear only at the (exponentially small) $O(\delta)$ level, suggesting that the solution is spatially uniform to all algebraic orders in θ. In other words, the structure of the core of the hot spot consists of an extremely weak chemico-acoustic field superimposed over a uniformly exploding atmosphere. Accordingly one seeks expansions of the form

(5.7a) $$u \sim \delta\, u_\delta(s,\sigma) + \ldots,$$

(5.7b) $$\Phi \sim \Phi_0(\sigma;\theta) + \delta\, \Phi_\delta(s,\sigma) + \ldots, \quad \text{for } \Phi = T,\ p,\ \rho, \text{ and } Y,$$

with the understanding that the Φ_0 contain all terms of algebraic orders. Substitution into (5.2) finds the Φ_0 satisfying the standard equations of constant-volume thermal explosion [8], i.e.,

(5.8a) $$\partial\rho_0/\partial\sigma = 0, \quad p_0 = \rho_0 T_0,$$

(5.8b) $$(1/\gamma)\,\rho_0\,\partial T_0/\partial\sigma = -\beta\rho_0\,\partial Y_0/\partial\sigma = W_0 \equiv \rho_0 Y_0 \exp[\theta(1-\sigma-1/T_0)].$$

The solution, subject to the matching conditions (5.5), is

(5.9a) $$\Phi_0 \sim \Phi_{00} + \theta^{-1}\,\Phi_{01} + \ldots, \quad \text{for } \Phi = T,\ p,\ Y \text{ and } \rho,$$

where

(5.9b) $T_{00} = p_{00} = (1-\sigma)^{-1}$, $Y_{00} = (1+\gamma\beta-T_{00})/(\gamma\beta)$, $\rho_{00} = 1$,

(5.9c) $T_{01} = -(1-\sigma)^{-2}\ell n\left[\gamma(1-\sigma)^2 Y_{00}\right]$, $\rho_{01} = \ell n(\gamma/B)$,

(5.9d) $p_{01} = T_{01} + \rho_{01}/(1-\sigma)$, $\beta\gamma Y_{01} = [\ell n(A_\gamma/\gamma) - T_{01}]$.

The structure functions Φ_δ satisfy, to leading order, the equations

(5.10a) $(s\partial/\partial s - \lambda)\rho_\delta + \rho_{00}\partial u_\delta/\partial s = 0$,

(5.10b) $\rho_{00}(s\partial/\partial s - \lambda)u_\delta + (1/\gamma)\partial p_\delta/\partial s = 0$,

(5.10c) $(s\partial/\partial s - \lambda)[\rho_{00}T_\delta - \{(\gamma-1)/\gamma\}p_\delta] = T_\delta W_{00}/T_{00}^2$,

(5.10d) $\rho_{00}(s\partial/\partial s - \lambda)Y_\delta = -T_\delta W_{00}/(\beta T_{00}^2)$,

(5.10e) $p_\delta - \rho_{00}T_\delta - T_{00}\rho_\delta = 0$,

where W_{00} is the leading term in the expansion for W_0, the latter having been defined in (5.8b). The use of the transformations

(5.11) $u_\delta = (1-\sigma)^{1/2}\,\hat{u}_\delta$, $s = \hat{s}(1-\sigma)^{-1/2}$,

reduces the set (5.10) to

(5.12a) $(\hat{s}\partial/\partial\hat{s} - \lambda)T_\delta + (\gamma-1)\partial\hat{u}_\delta/\partial\hat{s} = T_\delta$,

(5.12b) $(\hat{s}\partial/\partial\hat{s} - \lambda)(T_\delta - p_\delta) - \partial\hat{u}_\delta/\partial\hat{s} = 0$,

(5.12c) $(\hat{s}\partial/\partial\hat{s} - \lambda)\hat{u}_\delta + (1/\gamma)\partial p_\delta/\partial\hat{s} = 0$,

(5.12d) $\rho_\delta = (p_\delta - T_\delta)/T_{00}$,

(5.12e) $(\hat{s}\partial/\partial\hat{s} - \lambda)Y_\delta + \{1/(\beta\gamma)\}T_\delta = 0$.

Eqns. (5.12a-c) are identical to (4.16a-c) if T_δ, p_δ, $\hat{u}_\delta$ and $\hat{s}$ in the former are identified, respectively, with $\mathcal{T}_1^{(HC)}$, $\mathcal{P}_1^{(HC)}$, $\mathcal{U}_1^{(HC)}$ and s in the latter. Following the arguments of section

4.1, therefore, one is led to the solution

$$T_\delta = [\hat{A}(\sigma)/A]\mathcal{J}_1(\hat{s}), \tag{5.13a}$$

$$p_\delta = [\hat{A}(\sigma)/A]\mathcal{P}_1(\hat{s}) \tag{5.13b}$$

$$u_\delta = (1-\sigma)^{1/2}\,\hat{u}_\delta = (1-\sigma)^{1/2}[\hat{A}(\sigma)/A]\mathcal{U}_1(\hat{s}), \tag{5.13c}$$

where A is the constant introduced earlier in (4.18). The amplitude function $\hat{A}(\sigma)$ is unknown at this stage, and will be determined by matching with the main body of the hot spot, HB. So far we only know its initial value as a result of matching with the induction solution (4.32), i.e.,

$$\hat{A}(0) = A. \tag{5.14}$$

It is now a simple matter to solve (5.12d) for ρ_δ, and compute Y_δ by integrating (5.12e) subject to the regularity requirement. The resulting expressions are

$$\rho_\delta = (1-\sigma)[\hat{A}(\sigma)/A][\mathcal{P}_1(\hat{s})-\mathcal{J}_1(\hat{s})], \tag{5.15a}$$

$$\beta Y_\delta = [\hat{A}(\sigma)/A][\{(\gamma-1/\gamma)\mathcal{P}_1(\hat{s})-\mathcal{J}_1(\hat{s})]. \tag{5.15b}$$

Both the spatially uniform and the spatially-varying components of the expansions (5.7) are thus determined at leading orders, although the latter involve $\hat{A}(\sigma)$ which is still to be found. It is worth noting that the spatial structure of the solution is essentially the same as it was at induction-stage blowup; the scalings (5.11) simply reflect the temporal evolution of the acoustic speed.

As in the induction stage, the HC-solution breaks down for large s, the nonuniformity now occuring (see the expansion (4.21)) at $\theta\delta\hat{s}^{(2\gamma-1)/\gamma} = O(1)$. One is then led to the main body of the hot spot.

5.2 The Main Body of the Hot Spot, HB

Here the proper variables are ξ and σ where ξ is now related to x and $\hat{s}$ via the expressions

$$\xi = x\, e^{\theta\sigma\gamma/(2\gamma-1)} = (1-\sigma)^{-1/2}\,\hat{s}\, e^{\sigma\theta\mu}, \tag{5.16}$$

and μ was defined in (4.23). In the new variables the full equations (2.1) read

$$\theta^{-1}\rho_\sigma + (1-\mu)\xi\rho_\xi + e^{-\theta\sigma\mu}(\rho u)_\xi = 0, \tag{5.17a}$$

$$\rho e^{\theta\sigma\mu}[\theta^{-1}u_\sigma + (1-\mu)\xi u_\xi] + (1/\gamma)p_\xi + \rho u u_\xi = 0, \tag{5.17b}$$

$$\rho[\theta^{-1}T_\sigma + (1-\mu)\xi T_\xi] - \{((\gamma-1)/\gamma)[\theta^{-1}p_\sigma + (1-\mu)\xi p_\xi] + e^{-\theta\sigma\mu}u[\rho T_\xi - \{((\gamma-1/\gamma)p_\xi] = W, \tag{5.17c}$$

$$\rho[\theta^{-1}Y_\sigma + (1-\mu)\xi Y_\xi] + e^{-\theta\sigma\mu}u\rho Y_\xi = -(1/\beta)W, \tag{5.17d}$$

$$p = \rho T, \tag{5.17e}$$

where W retains the definition (5.3). The solution is subject to the following matching conditions imposed by HC:

$$T \sim T_{00} + \theta^{-1}[T_{01} - Q\xi^{(2\gamma-1)/\gamma}] + \ldots, \tag{5.18a}$$

$$p \sim T_{00} + \theta^{-1}[T_{01} + \rho_{01}/(1-\sigma) - Q\xi^{(2\gamma-1)/\gamma}] + \ldots, \tag{5.18b}$$

$$u \sim -e^{-\theta\sigma\mu}Q\xi^{(\gamma-1)/\gamma}\left[A_{\mathcal{U}}\mu\sigma + \theta^{-1}[A_{\mathcal{U}}\ell n\{(1-\sigma)^{1/2}\xi\} + B_{\mathcal{U}}]\right] + \ldots, \tag{5.18c}$$

(5.18d) $\rho \sim 1 + \theta^{-1}\ \rho_{01} + \ldots,$

(5.18e) $Y \sim Y_{00} + (\theta\beta\gamma)^{-1}\left[\ln(A_Y/\gamma) - T_{01} + Q\xi^{(2\gamma-1)/\gamma}\right] + \ldots,$ as $\xi \to 0.$

Here, Q is a quantity that appears frequently, and is defined by

(5.19a) $$Q(\sigma) \equiv \sigma\hat{A}(\sigma)\ (1-\sigma)^{(2\gamma-1)/\gamma},$$

with

(5.19b) $$Q(0) = \sigma A,$$

from (5.14). In obtaining the conditions (5.18) we have employed the expansions (4.21) and the solution (5.13); the variables with double subscripts are the spatially homogeneous functions appearing in (5.9). It turns out that compliance with these conditions also ensures temporal matching with the induction stage. The HB-solution is now sought in the form

(5.20a) $T \sim T_{00} + \theta^{-1}\ T_1^{(HB)}(\xi,\sigma) + \ldots,$

(5.20b) $p \sim T_{00} + \theta^{-1}\ p_1^{(HB)}(\xi,\sigma) + \ldots,$

(5.20c) $u \sim e^{-\theta\sigma\mu}\left[u_0^{(HB)}(\xi,\sigma) + \theta^{-1}\ u_1^{(HB)}(\xi,\sigma) + \ldots\right],$

(5.20d) $Y \sim Y_{00} + \theta^{-1}\ Y_1^{(HB)}(\xi,\sigma) + \ldots,$

(5.20e) $\rho \sim 1 + \theta^{-1}\ \rho_{01} + \ldots\ .$

(In the remainder of this section, the superscript HB will not be displayed explicitly.) Substitution into (5.17) shows that (5.17a)

is satisfied identically to $O(\theta^{-1})$. At O(1), (5.17b) reduces to

$$(1-\mu)\xi\partial u_0/\partial\xi - \mu u_0 = 0$$

whose solution subject to the matching requirement (5.18c) is

$$u_0 = \{((\gamma-1)/\gamma^2)\sigma Q\xi^{(\gamma-1)/\gamma}. \tag{5.21}$$

At $O(\theta^{-1})$, (5.17e) yields

$$p_1 = T_1 + p_{01}/(1-\sigma), \tag{5.22}$$

while (5.17c) reduces to

$$(1-\sigma)^{-2} + (1-\mu)\xi\partial T_1/\partial\xi - \{((\gamma-1)/\gamma)\left[(1-\sigma)^{-2} + (1-\mu)\xi\partial p_1/\partial\xi\right] = Y_{00}\exp[(1-\sigma)^2 T_1],$$

and, in view of (5.22), simplifies further to

$$(1-\sigma)^{-2} + (1-\mu)\xi\partial T_1/\partial\xi = \gamma Y_{00}\exp[(1-\sigma)^2 T_1]. \tag{5.23}$$

Its solution, consistent with the matching condition (5.18a), is

$$T_1 = T_{01} - (1-\sigma)^{-2}\ln\left[1 + (1-\sigma)^2 Q\xi^{(2\gamma-1)/\gamma}\right]. \tag{5.24}$$

With T_1 known, (5.22) defines p_1. In order to determine Y_1 consider (5.17d) at $O(\theta^{-1})$; it yields

$$-(\beta\gamma)^{-1}(1-\sigma)^{-2} + (1-\mu)\xi\partial Y_1/\partial\xi = (-1/\beta)Y_{00}\exp[(1-\sigma)^2 T_1].$$

When linearly combined with (5.23) the above equation leads to

$$\partial[T_1 + \beta\gamma Y_1]/\partial\xi = 0.$$

The matching condition (5.18e) then provides the following expression for Y_1:

(5.25) $$\beta\gamma Y_1 = \ell n(A_Y/\gamma) - T_1.$$

It now remains to determine u_1, and the function $Q(\sigma)$ (or, equivalently, $\hat{A}(\sigma)$). Both are obtainable from (5.17b) which, at $O(\theta^{-1})$, reads

(5.26) $$(1-\mu)\xi\partial u_1/\partial\xi - \mu u_1 = -\partial u_0/\partial\sigma - (1/\gamma)\partial p_1/\partial\xi.$$

With u_0 and p_1 known (see (5.21), (5.22) and (5.24)), the general solution of the above equation can be written as

(5.27) $$u_1 = \{(2\gamma-1)/\gamma\}\xi^{(\gamma-1)/\gamma}\left[K - \{(\gamma-1)/\gamma^2\}(\sigma Q)' \ell n\xi + (Q/\gamma)\ell n[\xi^{(2\gamma-1)/\gamma}/\{1+Q(1-\sigma)^2\xi^{(2\gamma-1)/\gamma}\}]\right],$$

where $K(\sigma)$ is the integration "constant". As $\xi \to 0$, u_1 has the asymptotic behavior

(5.28) $$u_1 \sim \{(2\gamma-1)/\gamma\}\xi^{(\gamma-1)/\gamma}\left[\left[-\{(\gamma-1)/\gamma^2\}(\sigma Q)'\right.\right.$$
$$\left.\left. + \{(2\gamma-1)/\gamma^2\}Q\right]\ell n\xi + K\right] + \ldots ,$$

which must agree with the $O(\theta^{-1})$ term in (5.18c). Matching the $\ell n\xi$ terms yields the differential equation

$$[\sigma Q(\sigma)]' = Q$$

whose solution, subject to (5.19b), is

(5.29a) $$Q = \alpha A,$$

or, equivalently,

(5.29b) $$\hat{A} = A(1-\sigma)^{-(2\gamma-1)/(2\gamma)}.$$

With Q determined, matching of the ξ-independent terms in (5.28) and (5.18c) yields K:

(5.30) $$K = (\alpha A/\gamma)[(1/2)\ell n(1-\sigma) - \{\gamma^2/(2\gamma-1)\}B_{\mathcal{U}}],$$

where the constant $B_{\mathcal{U}}$ was defined in equation 4.22. The HB-solution at the explosion stage is thus complete.

It is instructive to compare the solutions in the core and main body of the hot spot. In each the background field is that of a spatially homogeneous thermal explosion, but the superimposed spatially-varying field is quite different, both in amplitude and structure. In HC the

spatial component is exponentially small in amplitude but has a chemico-acoustic character; all disturbances to the background homogeneous field are of the same size. In HB the spatial variations in T, Y and p are $O(\theta^{-1})$, while those in u and ρ are exponentially small, i.e., the evolution is essentially due to chemistry, with gasdynamics playing a minor role.

As σ increases, T and p both increase, while Y decreases. Eventually, p and T peak when Y_{00}, the leading term in Y, vanishes. This happens at (see (5.9))

(5.31a) $$\sigma = \beta\gamma/(1+\beta\gamma),$$

and the peak values are

(5.31b) $$T \sim 1+\beta\gamma, \quad p \sim 1+\beta\gamma.$$

At the same time, the $O(\theta^{-1})$ term (in T, say; see (5.20a), (5.24) and (5.9c)) develops a logarithmic singularity, indicating breakdown of the solution and the end of the explosion stage.

5.3 The Frozen Region FR

This region remains essentially stationary, and hence plays no role during the explosion stage. For the sake of completeness, we give below the asymptotic form of the outer solution as $x \to 0$; these expressions are determined by combining (4.31) and (4.34):

(5.32a) $$T \sim 1 + \theta^{-1}\left[-((2\gamma-1)/\gamma)\ell n x - \ell n(A\alpha\gamma)\right] + \ldots,$$

(5.32b) $$p \sim 1 + \theta^{-1}\left[-\{(2\gamma-1)/\gamma\}\ell n x - \ell n(A\alpha B)\right] + \ldots,$$

(5.32c) $$u \sim \theta^{-1} A\alpha\, x^{(\gamma-1)/\gamma}\left[\{(2\gamma-1)/\gamma^2\}[\{-(\gamma-1)/\gamma\}\ell n x - \ell n(A\alpha)] - B_w\right] + \ldots .$$

Similar expressions can be written for ρ and Y. The important point to note is that this solution is unmatchable with that in HB; for example, to leading order, T is 1 in FR and $1/(1-\sigma)$ in HB. The reason is the emergence of the transition region TR in Figure 5, created by the receding hot spot. In this region T must vary, at leading order, from the outer value 1 to the inner value $1/(1-\sigma)$.

5.4 The Transition Region TR

This region, because of its passive character, will only be described very briefly. It is governed by the variables σ and X, where X is defined by

(5.33) $$x = e^{-\theta X}.$$

Matching with the neighboring regions is carried out at fixed σ, by setting

$$X = -\theta^{-1}\ell n x$$

as one approaches the outer region, and

$$X = \sigma(1-\mu) - \theta^{-1}\ell n \xi,$$

as the hot spot is approached. Therefore the range of X is

(5.34) $\quad 0 < X < \sigma(1-\mu)$;

recall that μ was defined in (4.23). From (5.20) one can easily conclude that leading-order matching with HB requires

(5.35a) $\quad T \sim 1/(1-\sigma) + \ldots$, as $X \to \sigma(1-\mu)$,

with analogous expressions for p and Y, while

(5.35b) $\quad \rho \sim 1, \; u \sim e^{-\theta X(\gamma-1)/\gamma} \{((\gamma-1)/\gamma^2)A\alpha\sigma.$

Therefore the solution is sought in the form

(5.36a) $\quad \Phi \sim \Phi_0^{(TR)} + \ldots$, for $\Phi = T, \; p, \; \rho$ and Y,

and

(5.36b) $\quad u \sim e^{-\theta X(\gamma-1)/\gamma} \; u_0^{(TR)} + \ldots$.

In the (X, σ) variables the full equations. (2.1) read

$$\rho_\sigma - (u\rho)_X \, e^{-\theta(\sigma-X)} = 0,$$
$$\rho\left[u_\sigma - uu_X \, e^{-\theta(\sigma-X)}\right] - (1/\gamma)p_X \, e^{-\theta(\sigma-X)} = 0,$$
$$\rho\left[T_\sigma - uT_X \, e^{-\theta(\sigma-X)}\right] - \{((\gamma-1)/\gamma)[p_\sigma - up_X \, e^{-\theta(\sigma-X)}\right] = \theta W,$$
$$\rho\left[Y_\sigma - uY_X \, e^{-\theta(\sigma-X)}\right] = -(1/\beta)\theta W,$$

$$p = \rho T,$$

where W retains the definition (5.3). Clearly, the solution is stationary, i.e., independent of σ to all algebraic orders. Specifically, the reaction term W is exponentially small since one expects $T < 1/(1-\sigma)$. The leading-order terms can then be determined simply by appealing to the matching conditions (5.35), and one finds that

$$(5.37a) \qquad T_0^{(TR)} = 1/[1-(1-\mu)^{-1}X],$$

with analogous expressions for p and Y, while

$$(5.37b) \qquad \rho_0^{(TR)} = 1, \; u_0^{(TR)} = \{(\gamma-1)/\gamma^2\}A\alpha\,(1-\mu)^{-1}X.$$

It is a simple matter to check that the above solution also matches with the outer expansions (5.32) as $X \to 0$.

The analysis of the Type-B explosion is thus complete.

6. The Type-I Reaction Center

In this section details are largely omitted and emphasis is on the results, since the treatment follows closely the Type-B analysis just concluded.

6.1 The Induction Stage

Figures 7(a-d) display the numerical solution of the induction problem. The graphs are self-explanatory. Similarity with Figures

1(a-d) is obvious, but two points of contrast are noteworthy. First, the temperature profile now has a rounded peak. Second, the boundary layer is thicker; this can be seen more clearly in Figure 8, where $T_1(x,t)/T_1(0,t)$ is plotted at the last successful time step for each of the two cases.

The boundary layer retains the form (4.8) and a two-sublayer strucure emerges once again. The expansions are

$$(6.1a)\qquad T \sim 1 + \theta^{-1}\left[-\ell n(\gamma\tau) - \tau\ell n\tau\,\{((\gamma-1)/\gamma)A + \tau\,\{-As^2 + C\} + \ldots\right] + \ldots,$$

$$(6.1b)\qquad p \sim 1 + \theta^{-1}\left[-\ell n(B\tau) - \tau\ell n\tau\,\{((\gamma+1)/\gamma)A + \tau\,[-As^2 + \{((\gamma+1)/(\gamma-1)\}C + A/\gamma] + \ldots\right] + \ldots,$$

$$(6.1c)\qquad u \sim \theta^{-1}\left[\tau\ell n\tau\,\{-2As/\gamma\} + \tau\,[2C/(\gamma-1) - A/\gamma\}]s + \ldots\right] + \ldots$$

in HC, and

$$(6.2a)\qquad T \sim 1 + \theta^{-1}\left[-\ell n(\gamma\tau) - \ell n(1+A\zeta^2) + \ldots\right] + \ldots,$$

$$(6.2b)\qquad p \sim 1 + \theta^{-1}\left[-\ell n(B\tau) - \ell n(1+A\zeta^2) + \ldots\right] + \ldots,$$

$$(6.2c)\qquad u \sim \theta^{-1}\left[\tau^{1/2}\ell n\tau\,\{-(2/\gamma)A\zeta + \tau^{1/2}\,[-(2/\gamma)A\zeta\,\ell n(1+A\zeta^2) + \{2C/(\gamma-1) - A/\gamma\}\zeta\} + \ldots\right] + \ldots,$$

in HB. The constants A, B and C are to be determined by matching with the outer solution as before. The spatial coordinate ζ in HB is defined by

$$(6.3)\qquad \zeta = x/\tau^{1/2},$$

implying that the boundary layer is now $O(\varepsilon^{1/2})$ thick, and hence thicker than the $O(\varepsilon^{\gamma/(2\gamma-1)})$ Type-B layer. The finding of Figure 8 is thus confirmed.

It turns out further that the HB-solution is uniformly valid all the way to $\zeta = 0$, so that the core of the hot spot is, in fact, superfluous.

For smooth merging with the boundary layer the outer, numerically computed solution is required to have the asymptotic form

$$(6.4a) \qquad T \sim 1 + \theta^{-1}\,[-2\ell nx - \ell n(\gamma A) + \ldots] + \ldots,$$

$$(6.4b) \qquad p \sim 1 + \theta^{-1}\,[-2\ell nx - \ell n(AB) + \ldots] + \ldots,$$

$$(6.4c) \qquad u \sim \theta^{-1}\,[-4(A/\gamma)x\ell nx + \{-2(A/\gamma)\ell nA + 2C/(\gamma-1) - A/\gamma\}x + \ldots] + \ldots, \text{ as } x \to 0.$$

This behavior was confirmed, and the constants A, B and C computed, by comparing the numerical solution with the above expansions. The remaining variables ρ_1 and Y_1 can be determined as before, by appealing to the first member of (3.2c), and (3.2d).

6.2 The Explosion Stage

The analysis proceeds as in section 5.2. The appropriate coordinates are σ and ζ, and the requirement of matching with HC is replaced by the condition of regularity at $\zeta = 0$. The solution turns out to be

$$(6.5a) \qquad T \sim T_{00} + \theta^{-1}\,\left[T_{01} - (1-\sigma)^{-2}\ell n\{1+A\zeta^2\}\right] + \ldots,$$

$$p \sim T_{00} + \theta^{-1}\left[T_{01} - (1-\sigma)^{-2}\ell n\{1+A\zeta^2\} + \rho_{01}/(1-\sigma)\right] + \ldots, \tag{6.5b}$$

$$u \sim e^{-\theta\sigma/2}\,[2A\zeta/\{\gamma(1-\sigma)\}] + \ldots \tag{6.5c}$$

$$\rho \sim 1 + \theta^{-1}\,\rho_{01} + \ldots, \tag{6.5d}$$

$$Y \sim Y_{00} + (\theta\beta\gamma)^{-1}\left[\ell n(A_Y/\gamma) - T_{01} + (1-\sigma)^{-2}\ell n\{1+A\zeta^2\}\right] + \ldots, \tag{6.5e}$$

where the constant A_Y appearing in (6.5e) was defined in (4.38). The doubly subscripted quantities correspond to the spatially homogeneous explosion, and were introduced in (5.9). The explosion stage peaks just as it did for Type-B, and the remarks at the end of section 5.2 remain valid. Finally, the TR-analysis of section 5.4 carries over, with obvious modifications.

7. Concluding Remarks

The spatial structure and temporal evolution of a localized thermal explosion in a confined material have been described mathematically. A local, rather than a spatially uniform explosion, occurs as a result of an inhomogeneity, here modelled by a slightly nonuniform initial temperature. Attention is confined to what may be called the fast-reaction limit, characterized by the initial induction time of the reaction being comparable to the initial acoustic time, so that diffusion plays no role. This limit can be achieved if the initial temperature of the unreacted material has been raised to a sufficiently high level, perhaps by the passage of a strong shock. By contrast, the slow-reaction limit would correspond to the induction time and the conduction time being of the same order. The latter problem was the subject of Poland and Kassoy's investigation [8].

The explosion is shown to develop in two distinct stages. The first stage is induction, characterized by small perturbations about a spatially uniform state, where the primary interaction is between linearized acoustics and weak but nonlinear chemical heating. Chemical amplification leads to localized thermal runaway, or blowup of the perturbations, at a time and location determined by the initial and boundary conditions. The spatial structure at blowup is essentially self-similar, depending only weakly on the initial and boundary conditions.

Induction is followed by explosion, characterized by O(1) variations in the state of the material. The characteristic chemical

time in the hot spot plunges dramatically. The corresponding acoustic time drops as well, but not nearly as rapidly, so that hot-spot formation is dominated by chemical heating. There is no time for expansion, with the result that changes in the velocity and density fields are negligible. Thus the material explodes locally at essentially constant-density conditions, with little change in the spatial structure that it inherited at runaway. The explosion stage ends when temperature and pressure within the hot spot have peaked, their final values being exactly the same to leading order, as in the spatially homogeneous case.

The main structural features of the evolution of the reaction center can be summarized in a simple way by giving only the leading-order results in the explosion stage. For $x \to 0$ and $t \to t_e$ the evolution of the center is described approximately by the formulas

$$T = p = 1/[1+\theta^{-1}\ell n(t_e-t)],\quad \rho = 1,\quad u = 0, \qquad 0 < x < (t_e-t)^{(1-\mu)}, \tag{7.1}$$

in the hot spot, and,

$$T = p = 1/[1+\theta^{-1}\ell n\, x\,(1-\mu)^{-1}],\quad \rho = 1,\quad u = 0, \qquad x > (t_e-t)^{(1-\mu)}, \tag{7.2}$$

in the transition region, for

$$0 < t < t_e - \exp[-\theta((1+\beta)/(\beta\gamma))].$$

The value of μ is $(\gamma-1)/(2\gamma-1)$ for type-B and 1/2 for type-I. Consistent with our previous discussion, the region of maximum temperature and pressure shrinks as the explosion proceeds. A sketch of the evolution of temperature and pressure according to these formulas is shown in Fig. 9.

The subsequent expansion of the hot, highly compressed material, and the eventual development of a detonation, are currently under study.

Acknowledgments

Parts of this work were carried out during visits to ICASE (by A. K. Kapila) and the Los Alamos National Laboratories (by A. K. Kapila and D. S. Stewart). The hospitality and financial support of the institutions is gratefully acknowledged. The authors also thank John Bdzil (LANL) for his encouragement and comments.

FIGURE CAPTIONS

1. A schematic of the temperature profiles for the Type-B (sharp peaked) and the Type-I (round-peaked) explosion.
2. Type-B induction-stage profiles for (a) T_1, (b) p_1, (c) u_1 and (d) ρ_1, for γ=1.4, a=0.5, ℓ=0.8 and initial data given by eqn. (3.3). The profiles are plotted at (i) t=0, (ii) t=0.2, (iii) t=0.4, (iv) t=0.43, (v) t=0.442, (vi) t=0.44625. Estimate of blowup time is t_e = 0.446890.
3. Plot of $\exp[-T_1(0,t)]$ for Type-B problem.
4. Type-B plots of $T_1(0,t)$, $p_1(0,t)$ and $u_1(0,t)$.
5. A schematic of the spatial zones at and beyond blowup. H: Hot spot, HC: Core of the hot spot, HB: Main body of the hot spot, FR: Frozen region, TR: Transition region. Not to scale (The t-scale is cosiderably stretched).
6. Profiles of structure functions $\mathcal{J}_1$, $\mathcal{Q}_1$ and $\mathcal{U}_1$ for $\mathcal{J}_1(0)$=1.
7. Type-I induction-stage profiles for (a) T_1, (b) p_1, (c) u_1 and (d) ρ_1, for γ=1.4, a=0.5, ℓ=0.8 and initial data given by eqn. (3.3). The profiles are plotted at (i) t=0, (ii) t=0.2, (iii) t=0.4, (iv) t=0.422, (v) t=0.432, (vi) t=0.435875. Estimate of blowup time is t_e = 0.435880.
8. Plots of $T_1(x,t)/T_1(0,t)$ at the last integration step for (a) Type B, and (b) Type I.
9. The evolution of temperature and pressure for the reaction center for times close to t_e according to formulas (7.1) and (7.2).

REFERENCES

1. Urtiew, P. A. and Oppenheim, A. K. (1966) Experimental observations of the transition to detonation in an explosive gas, Proc. Roy. Soc. A 295, 13-28.

2. Campbell, A. W., Davis, W. C. and Travis, J. R. (1961) Shock-initiation of detonation in liquid explosives, Phys. Fluids 4, 498-510.

3. Zajac, L. J. and Oppenheim, A. K. (1971) Dynamics of an explosive reaction center, AIAA J. 9, 545-553

4. Meyer, J. W. and Oppenheim, A. K. (1972) Dynamic response of a plane-symmetrical exothermic reaction center, AIAA J. 10, 1509-1513.

5. Stewart, D. S. (1986) Shock initiation of homogeneous and heterogeneous condensed-phase explosives with a sensitive rate, Comb. Sci. Tech. 48, 309-330.

6. Clarke, J. F. and Cant, R. S. (1984) Non-steady gasdynamic effects in the induction domain behind a strong shock wave, Progress in Aeronautics and Astronautics 95, 142-163.

7. Jackson, T. L. and Kapila, A. K. (1985) Shock-induced thermal runaway, SIAM J. Appl. Math. 45, 130-137.

8. Poland, J. and Kassoy, D. R. (1983) The induction period of a thermal explosion in a gas between infinite parallel plates, Combustion and Flame 50, 259-274.

9. Williams, F. A. (1985) Combustion Theory, Benjamin Cummings Publishing Company.

10. Kassoy, D. R. (1976) Extremely rapid transient phenomena in combustion, ignition and explosion, in Asymptotic Methods and Singular Perturbations, R. E. O'Malley, Jr., ed.,SIAM-AMS Proceedings 10, 61-72.

Appendix

The setup (4.8), employed in the text for analyzing the spatial structure of blowup, is based on the numerical observation that both T_1 and p_1 exhibit identical, $-\ell n\tau$ behavior as $\tau \to 0$. This observation, found to hold for all the numerical runs undertaken, implies that blowup is a constant-density process, since density perturbation $\rho_1 = p_1 - T_1$ remains bounded.

Let us now consider the possibility that for some initial conditions, blowup lies partway between a constant-density and a constant-pressure process, and ask whether a self-similar structure consistent with this notion exists. Accordingly, we replace (4.8) by

$$T_1 = -\ell n\tau + \mathcal{J}(s) , \tag{A.1a}$$

$$p_1 = -\Lambda \ell n\tau + \mathcal{G}(s) , \tag{A.1b}$$

$$u_1 = \mathcal{U}(s) , \tag{A.1c}$$

where

$$0 < \Lambda < 1.$$

The case $\Lambda = 0$ corresponds to a constant-pressure situation, and $\Lambda = 1$ to the constant-density case already discussed. Substitution into (4.7), followed by some rearrangement, yields the leading-order structure equations

$$s(1-s^2)\mathcal{J}' + [1-s^2-((\gamma-1)/\gamma)\Lambda] = (1-\gamma s^2)\exp[\mathcal{J}], \tag{A.2a}$$

(A.2b) $$(1-s^2)\rho' = s[\Lambda - \gamma \exp \mathcal{J}],$$

(A.2c) $$\gamma(1-s^2)\mathcal{U}' = \gamma \exp \mathcal{J} - \Lambda.$$

The transformation

(A.3) $$\mathcal{J} = -\ell n F$$

reduces (A.2a) to the linear equation

(A.4) $$s(1-s^2)F' - [[1-s^2-((\gamma-1)/\gamma)\Lambda]F = 1-\gamma s^2.$$

Once F is known, $\mathcal{U}$ and ρ can be computed from (A.2b,c).

Equation (A.3) has singular points at s = 0 and 1. It can be shown that integration can remove at most one singularity, thereby yielding solutions which are singular either at 0 or at 1. Such solutions can evolve only from very special, singular initial conditions, and are therefore unacceptable if the initial data are smooth. The only regular solution is the constant

$$F = \gamma,$$

which requires

$$\Lambda = 1,$$

corresponding to the constant-density blowup already discussed.

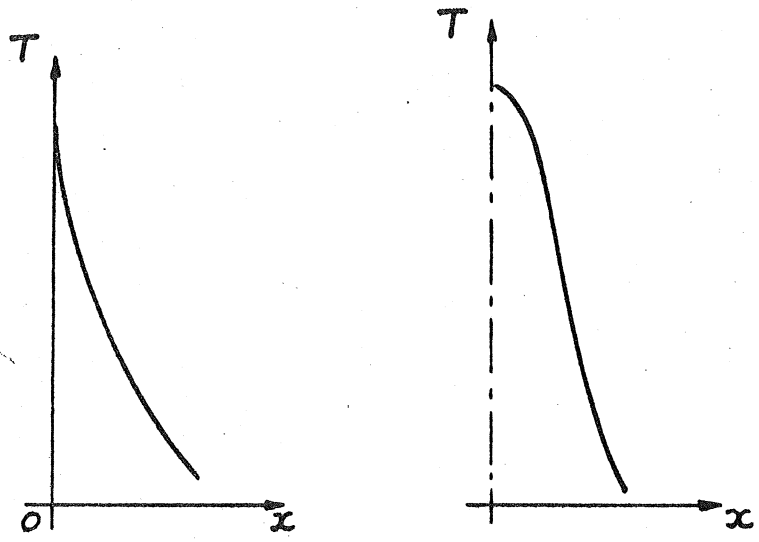

FIG. 1

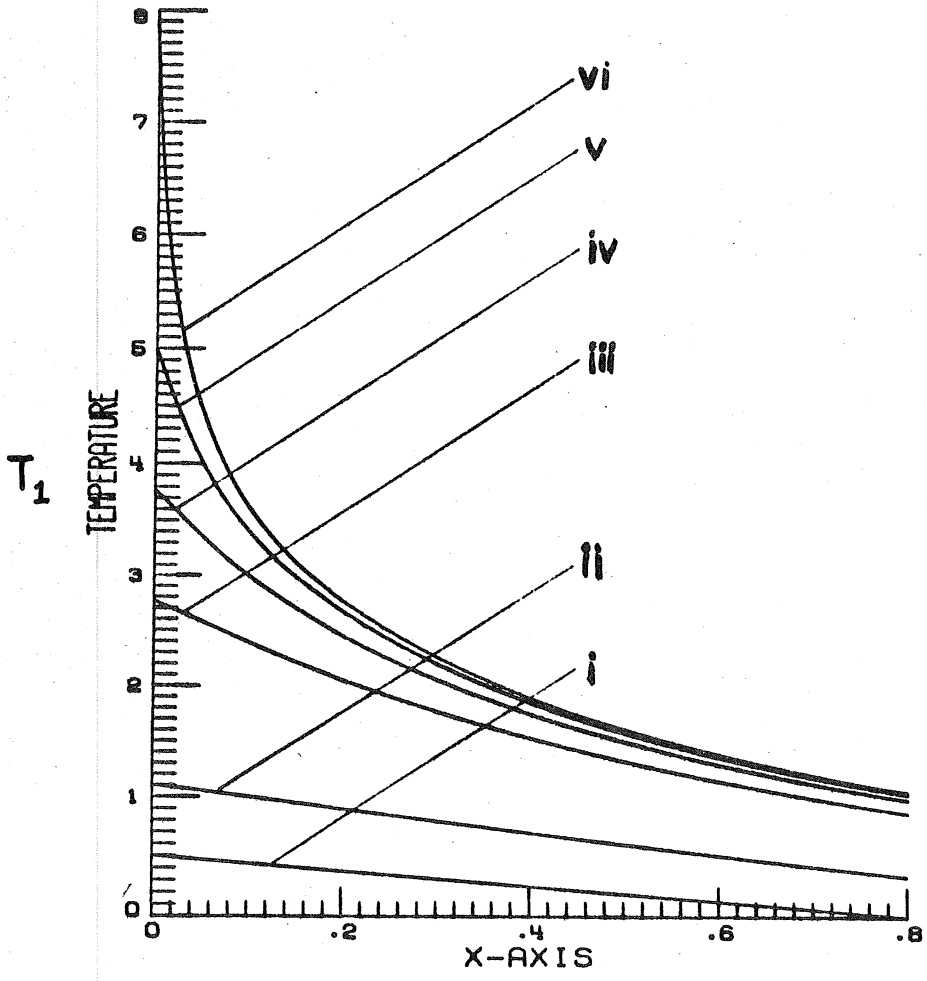

Fig. 2(a)

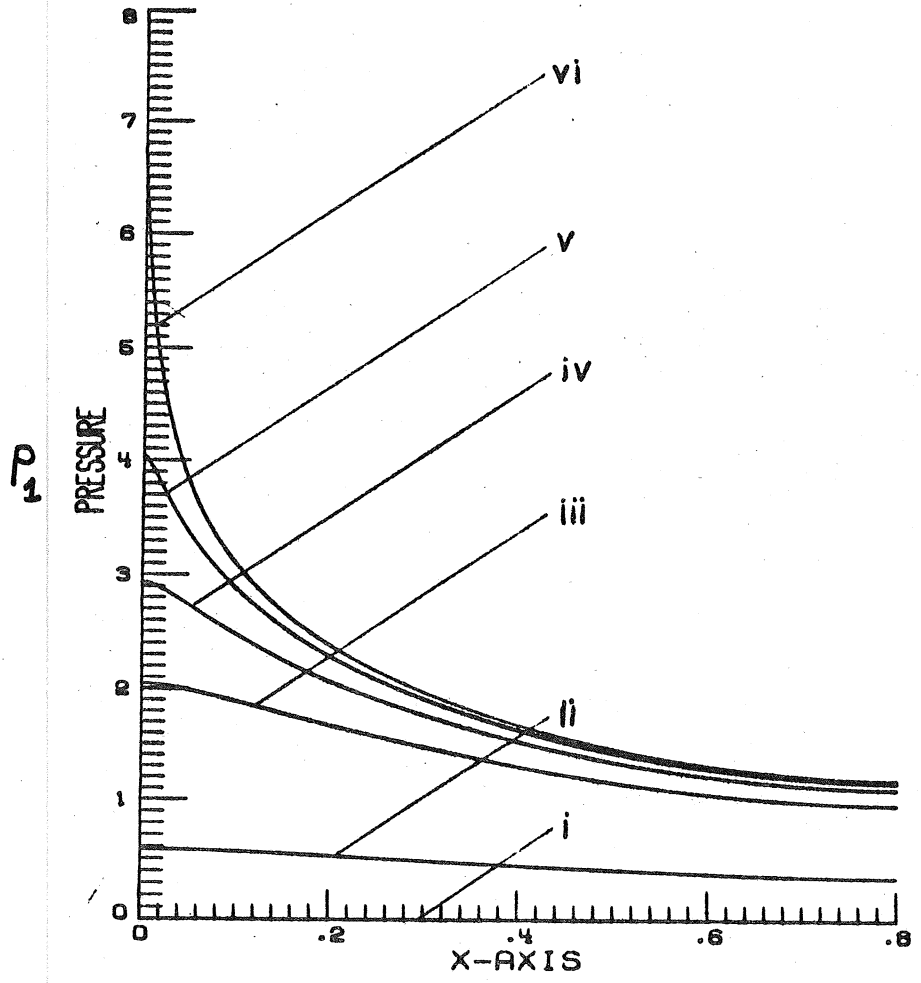

Fig. 2(b)

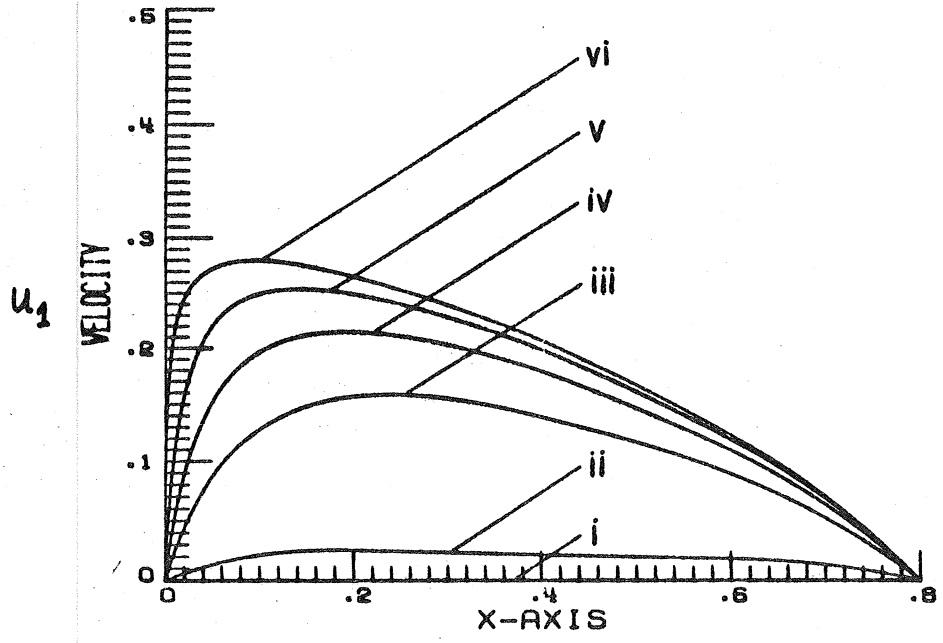

Fig. 2(c)

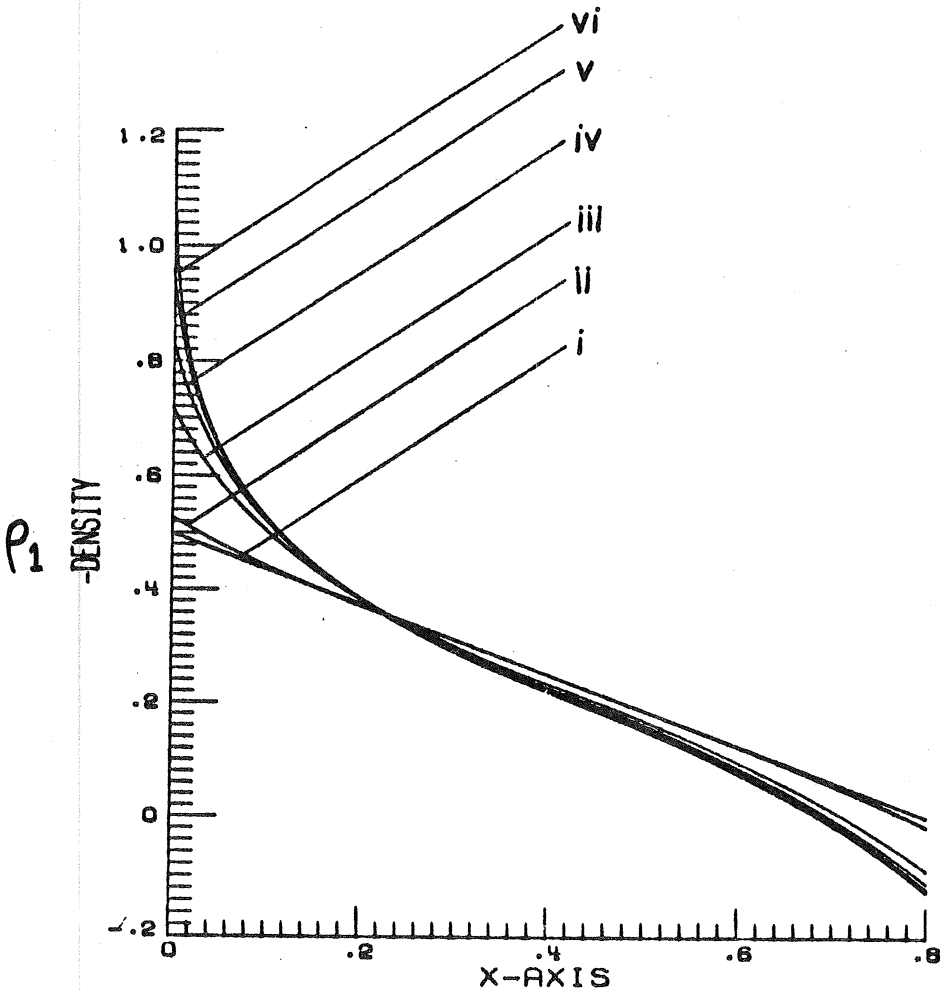

Fig. 2(d)

Fig. 3

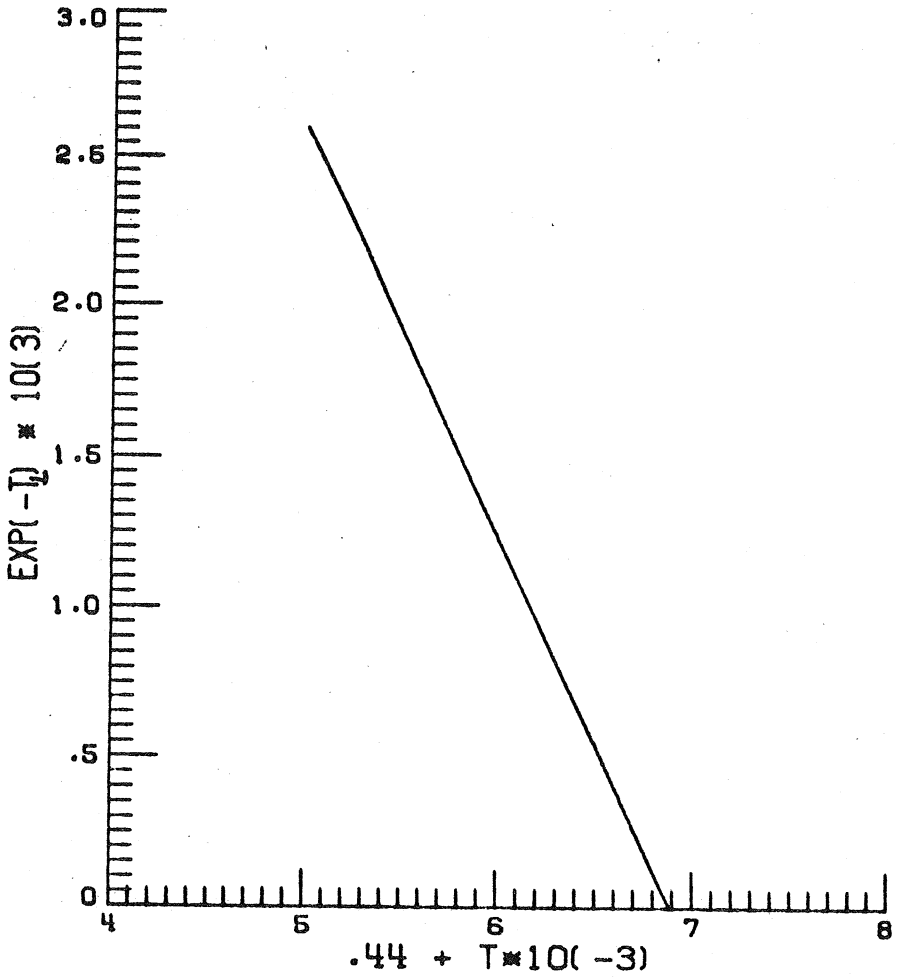

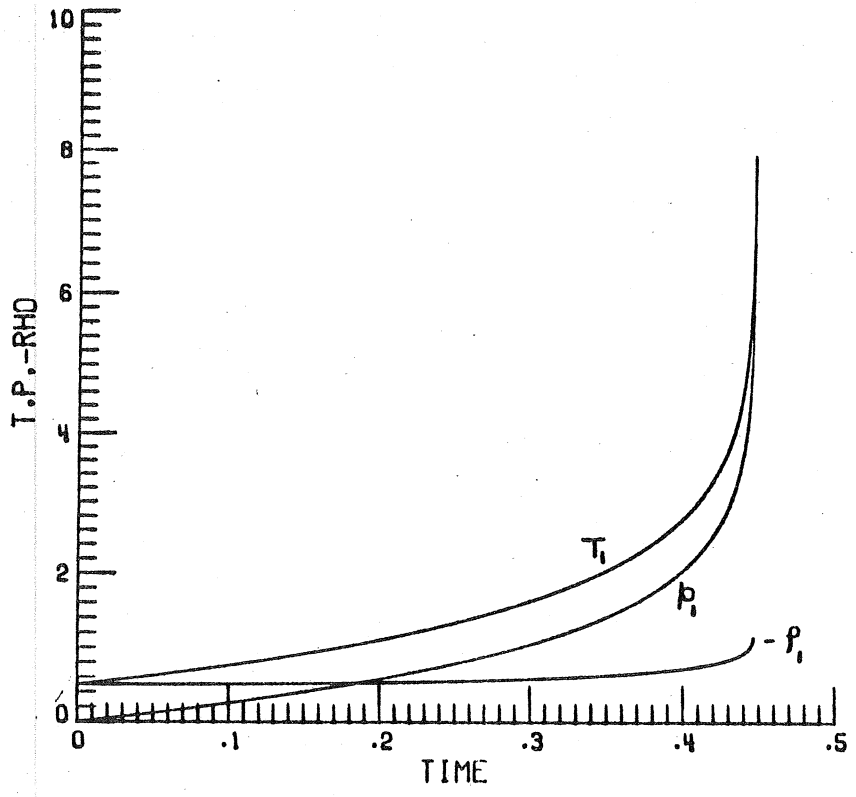

Fig. 4

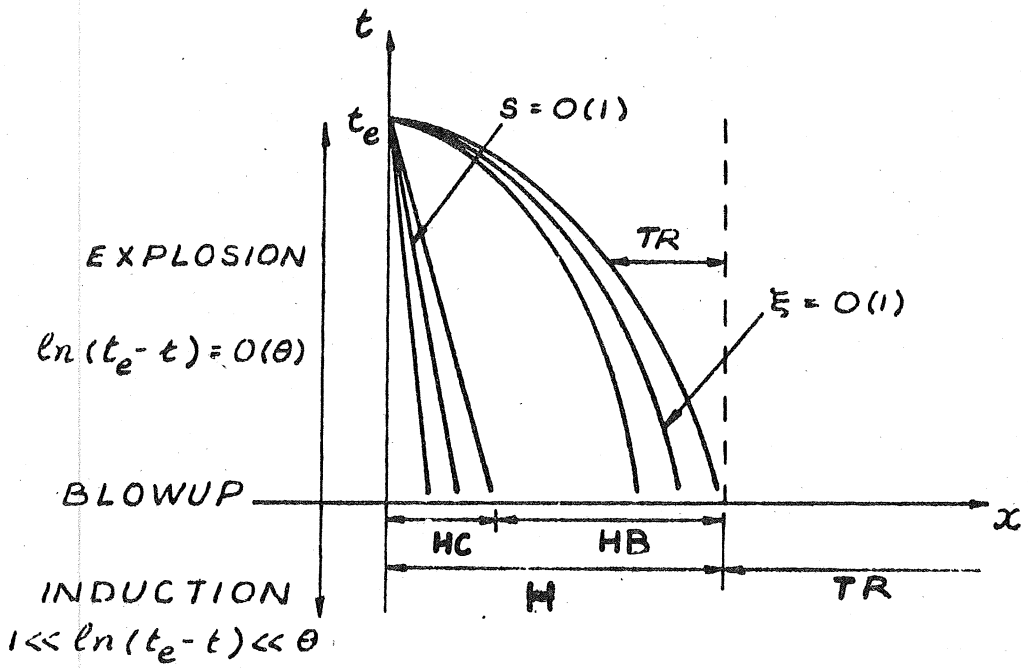
t
t_e
S = O(1)
TR
ξ = O(1)
EXPLOSION
$\ln(t_e - t) = O(\theta)$
BLOWUP
x
HC
HB
H
TR
INDUCTION
$1 \ll \ln(t_e - t) \ll \theta$

Fig. 5

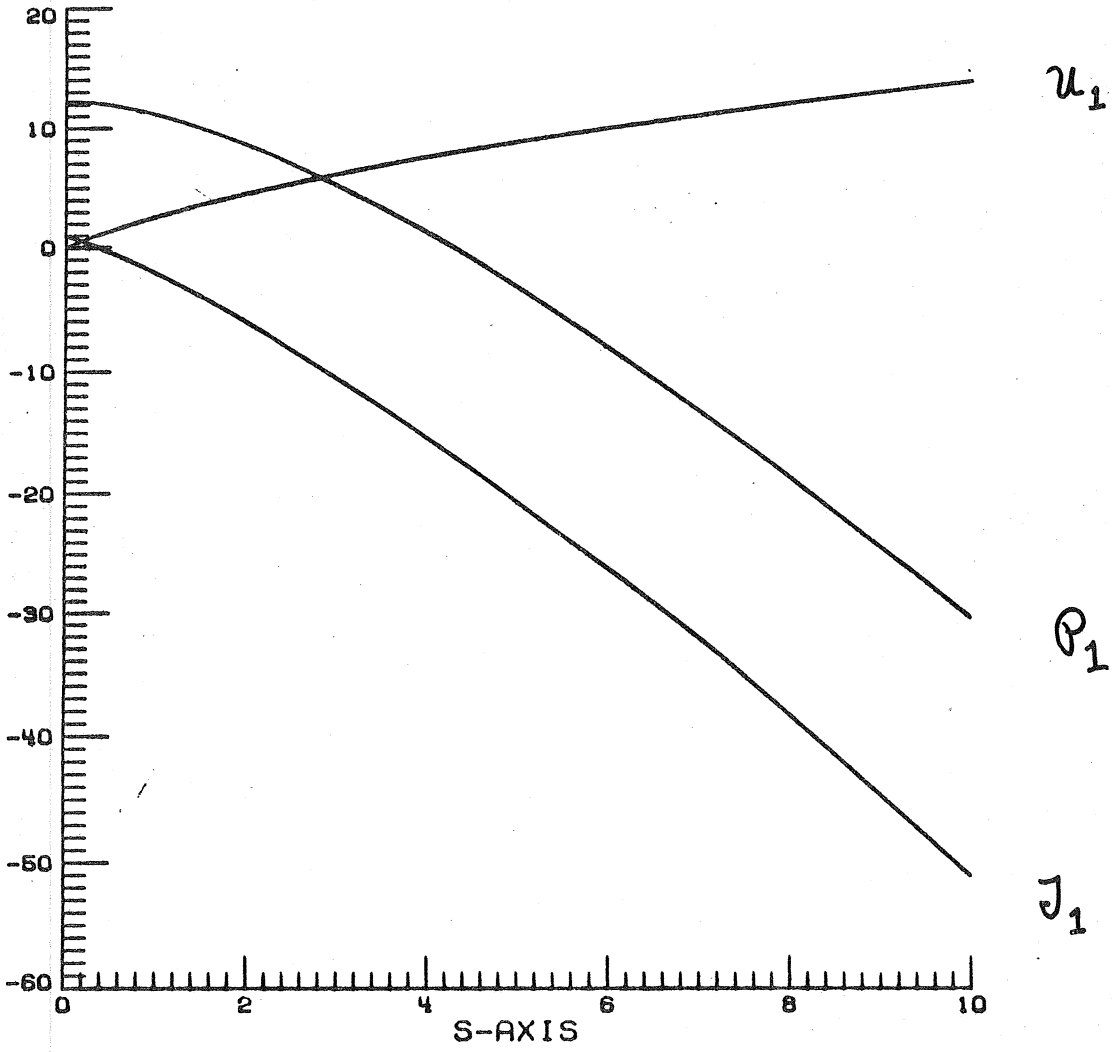

Fig. 6

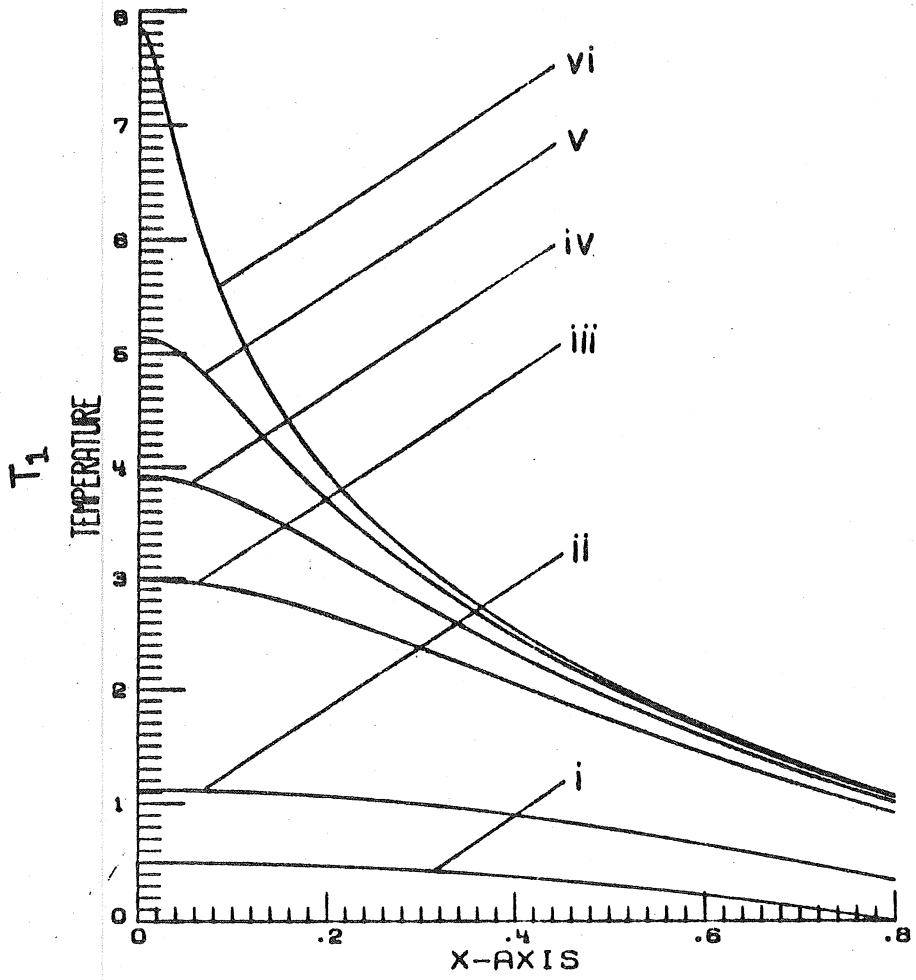

Fig. 7(a)

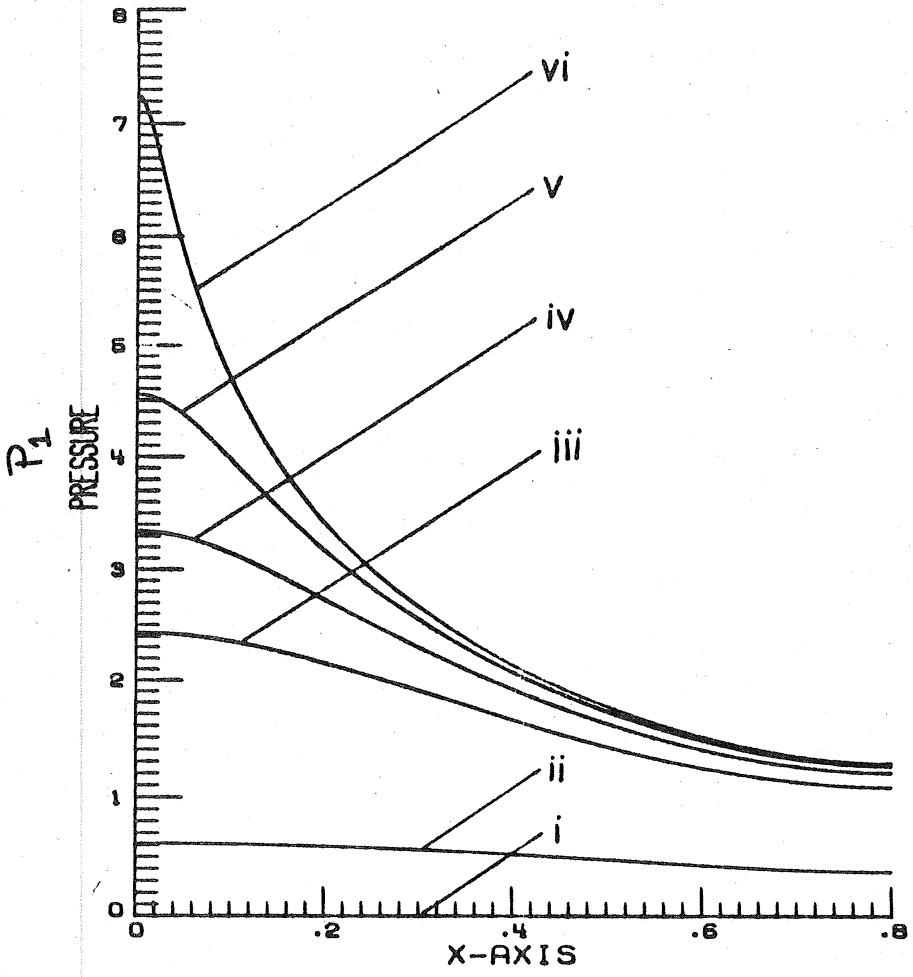

Fig. 7(b)

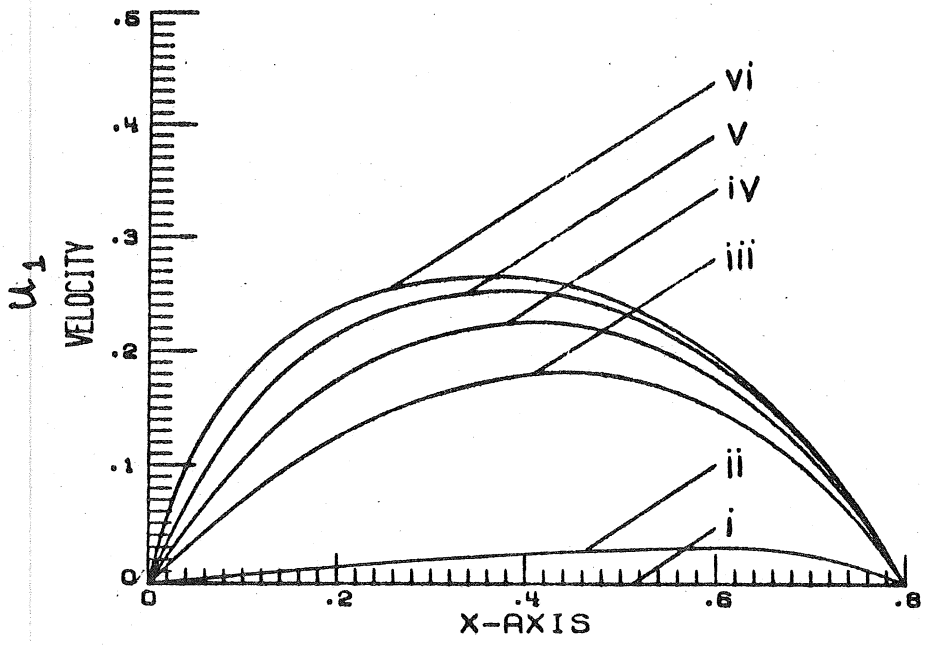

Fig. 7(c)

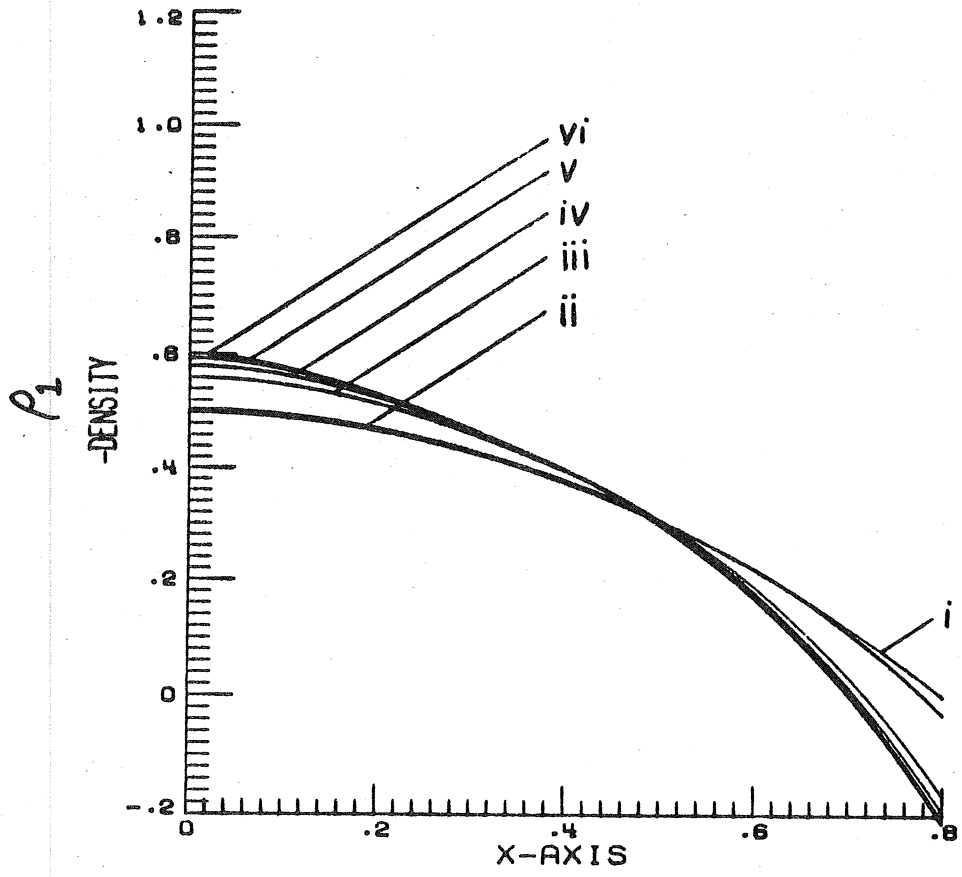

Fig. 7(d)

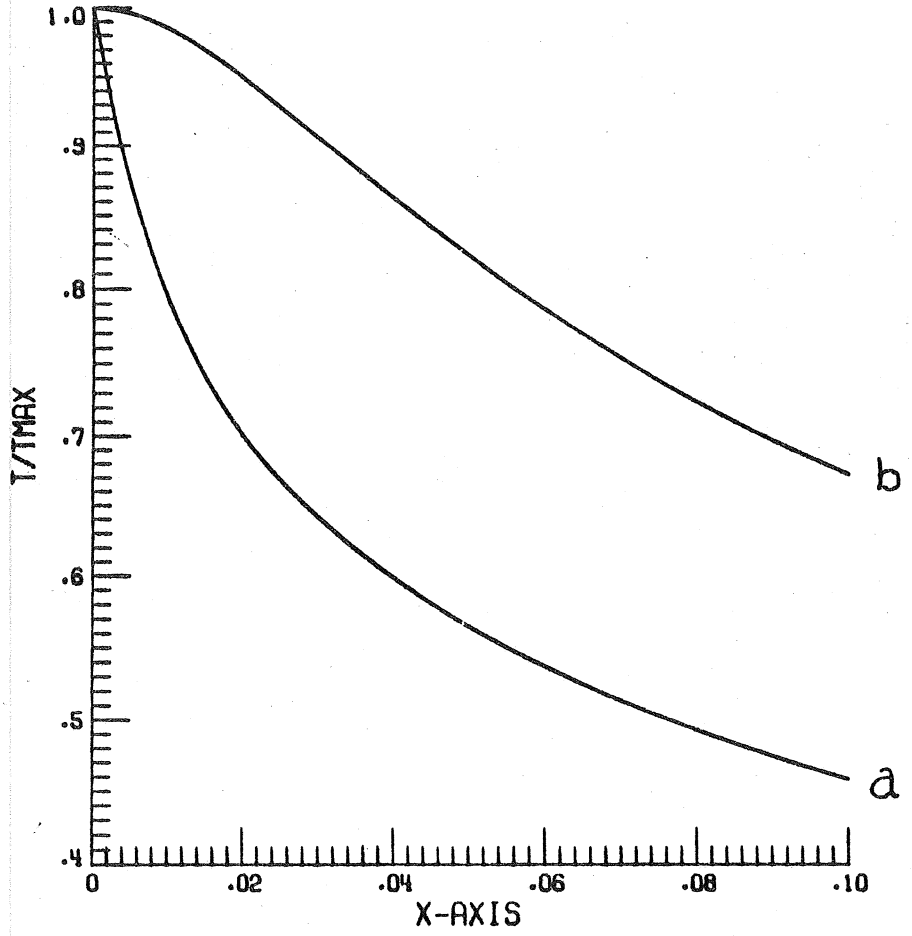

Fig. 8

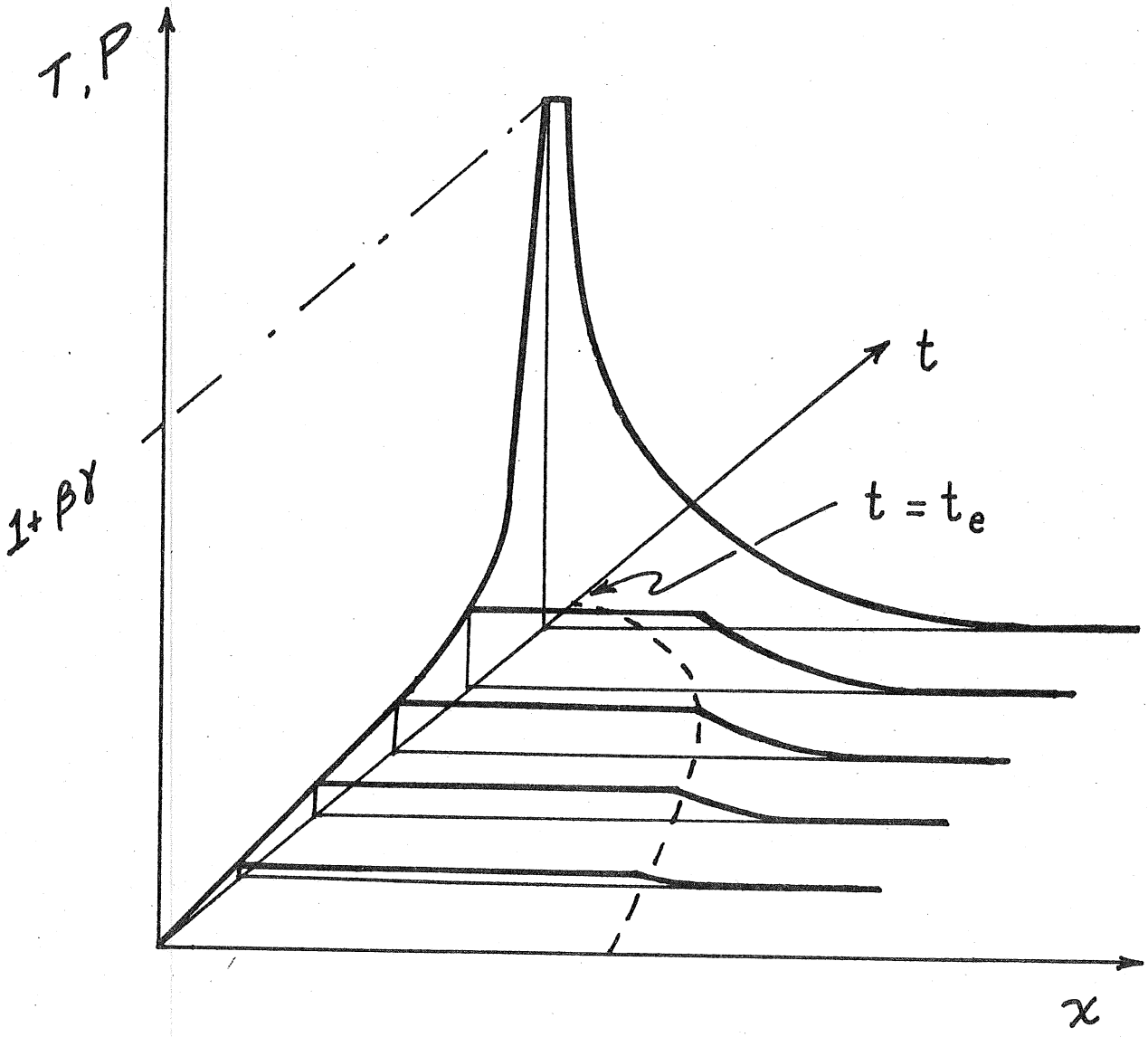

Fig. 9